Spectral and Dynamical signatures of many-body localization

Google quantum hardware

Pedram Roushan

KITP, May 1st 2019

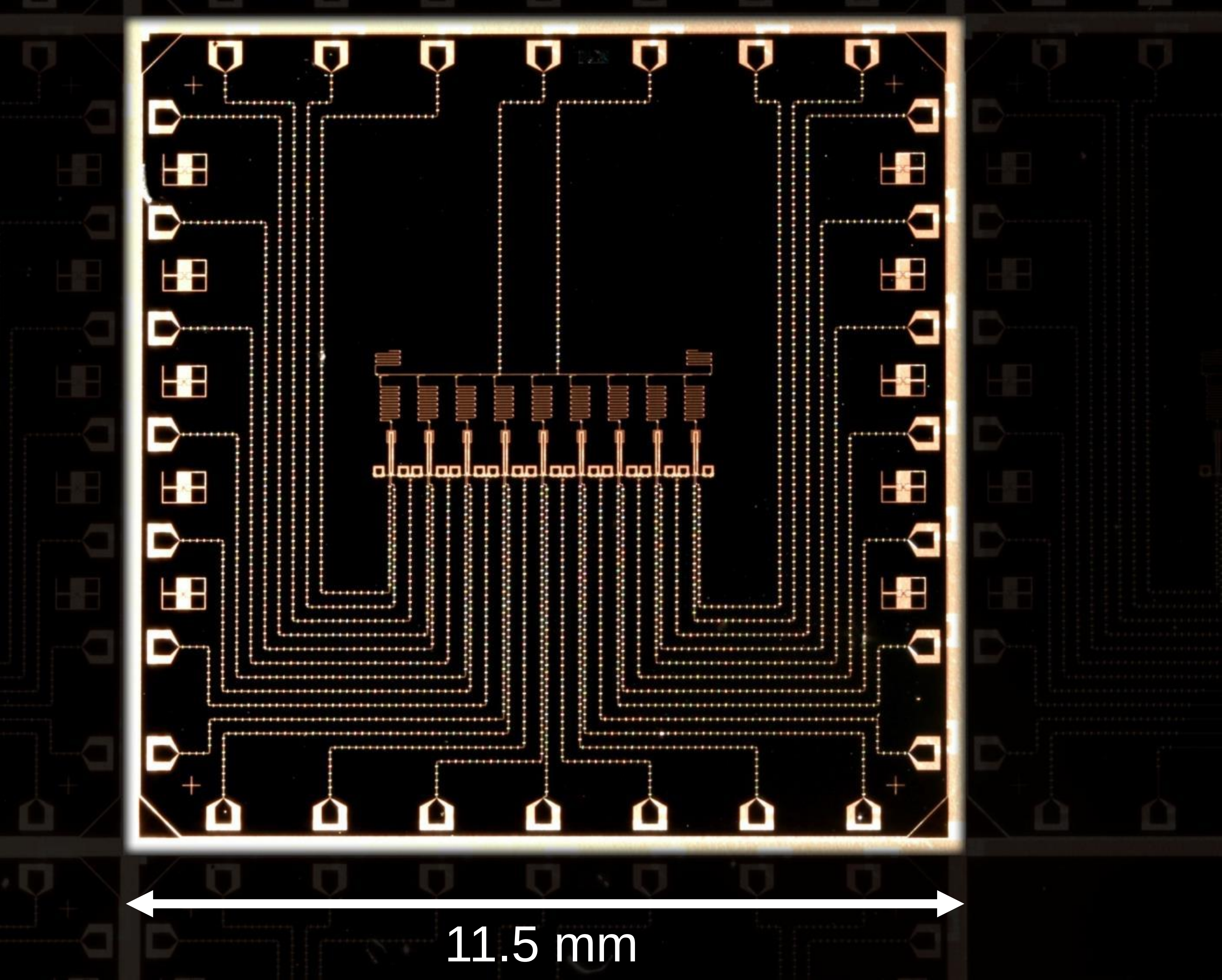

An optical micrograph of the 9-qubit chip.

1D chain of 9 qubits

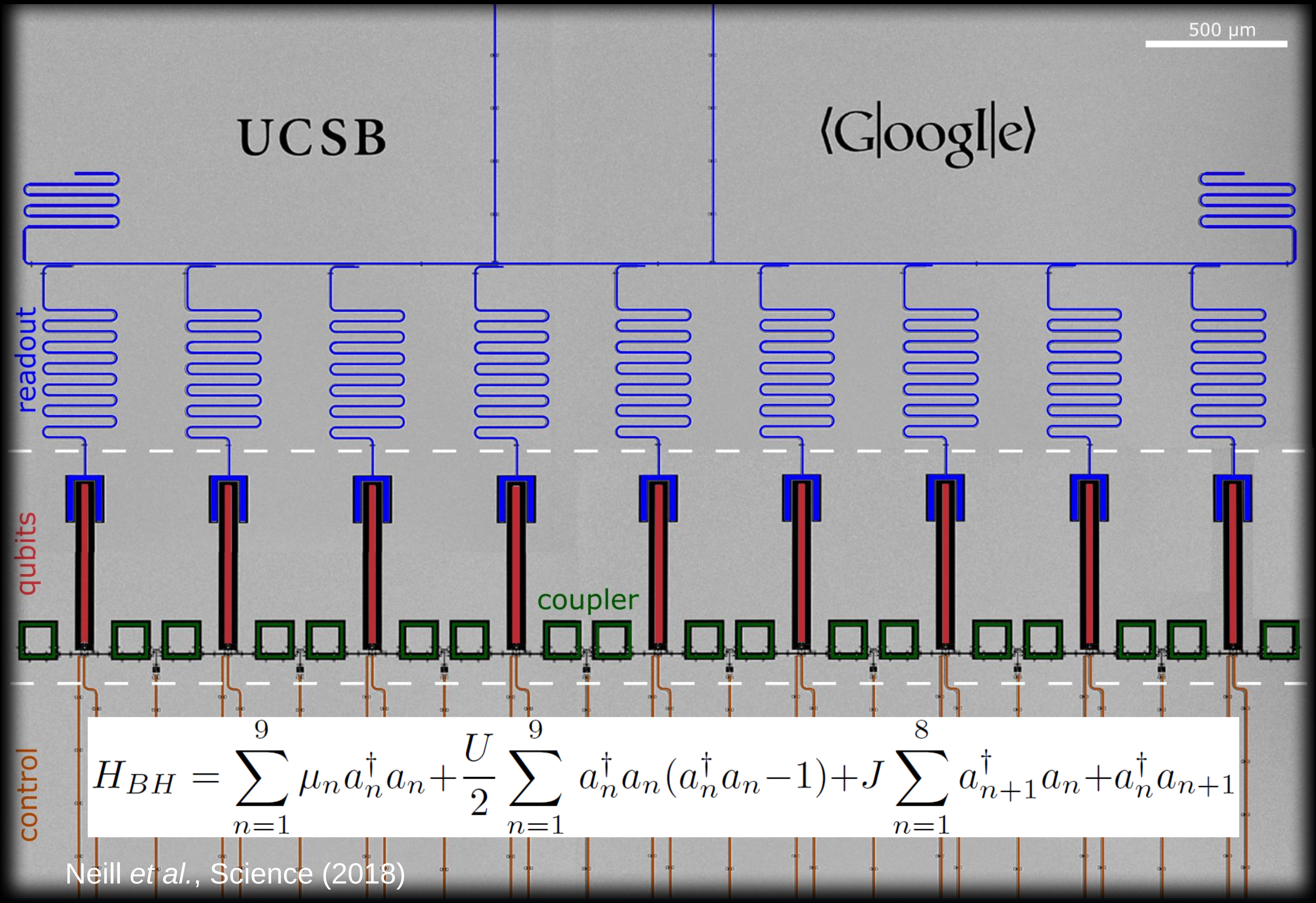

$$H_{BH} = \sum_{n=1}^{9} \mu_n a_n^\dagger a_n + \frac{U}{2} \sum_{n=1}^{9} a_n^\dagger a_n (a_n^\dagger a_n - 1) + J \sum_{n=1}^{8} a_{n+1}^\dagger a_n + a_n^\dagger a_{n+1}$$

Neill *et al.*, Science (2018)

Two coupled qubits

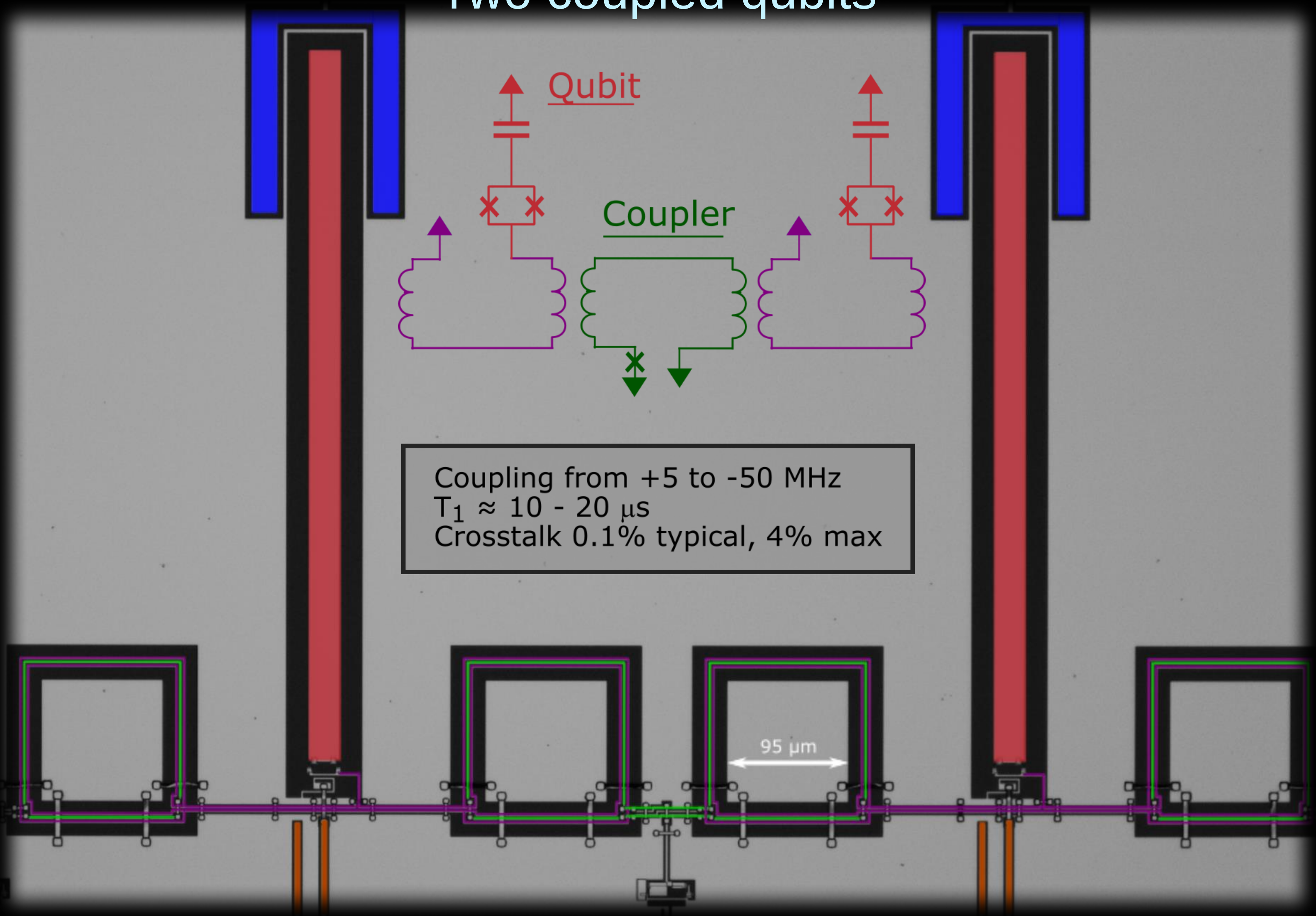

The gmon (Jmon) architecture

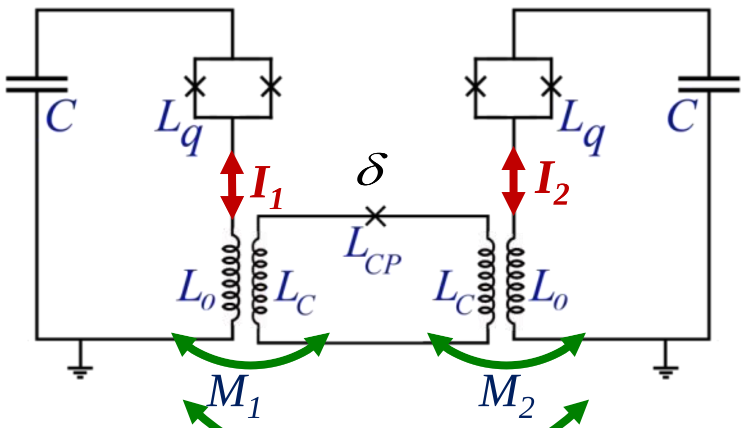

$$M = \frac{M_1 M_2}{L_{CP} + 2L_C}$$

$$\omega_1 = \omega_0 \left(1 - \frac{M}{2L_q}\right)$$

$$\omega_2 = \omega_0 \left(1 + \frac{M}{2L_q}\right)$$

$$J \equiv \frac{\omega_2 - \omega_1}{2}$$

$$J / \omega_0 = \frac{M_1 M_2}{2L_q} \frac{\cos(\delta)}{2L_0 \cos(\delta) + L_C}$$

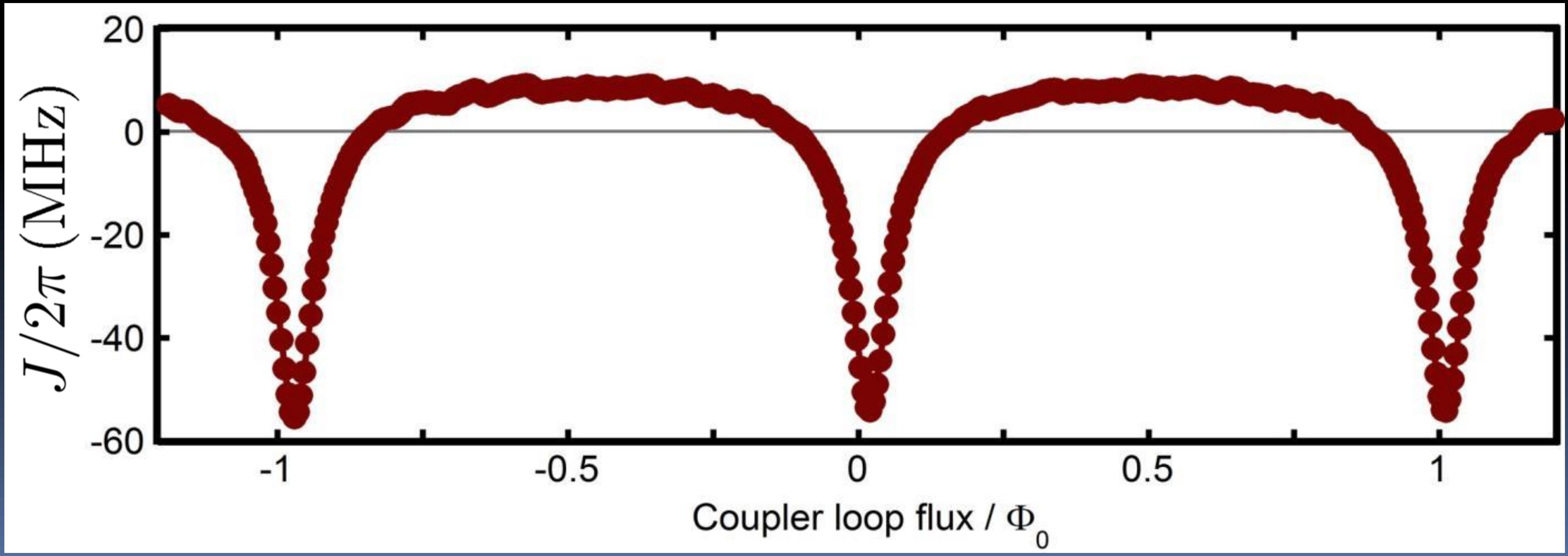

Can an isolated system act as its own heat bath ?

Fundamental assumption of statistical mechanics:
All micro-states associated with a given macro-states have equal probability.

t=0 (away from equilibrium)

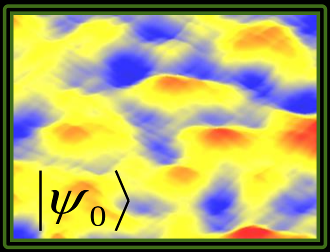

$|\psi_0\rangle$

$$|\psi\rangle = e^{-iHt}|\psi_0\rangle$$

t (in equilibrium)

$$\rho = e^{-\beta H}$$

Non-interacting particles

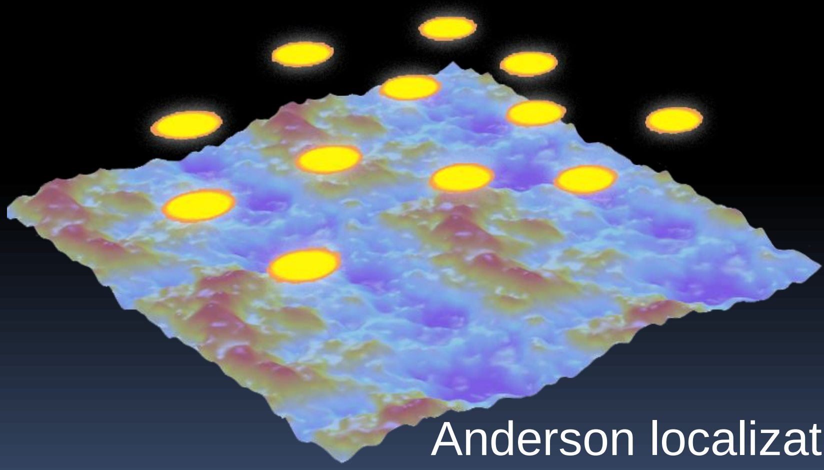

Anderson localization

Interacting particles

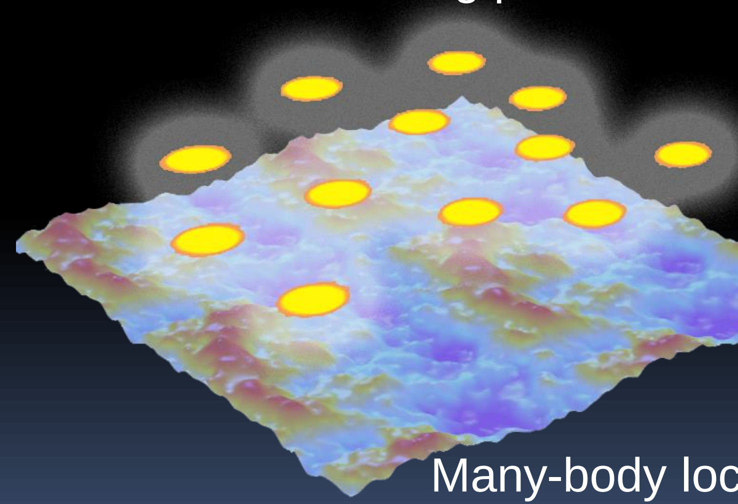

Many-body localization

P. W. Anderson (1958)
Absence of diffusion in certain random lattices

Basko, Aleiner, and Altshuler (2006)
Metal-insulator transition in a weakly interacting many-electron system with localized single-particle states

Recent studies of many-body localization

[1] D.M. Basko, I.L. Aleiner, and B.L. Altshuler, "Metal-insulator transition in a weakly interacting many-electron system with localized single-particle states," Annals of Physics **321**, 1126–1205 (2006).
[2] R. Nandkishore and D. A. Huse, "Many-body localization and thermalization in quantum statistical mechanics," Annual Review of Condensed Matter Physics **6**, 15–38 (2015).
[3] E. Altman and R. Vosk, "Universal dynamics and renormalization in many-body-localized systems," Annual Review of Condensed Matter

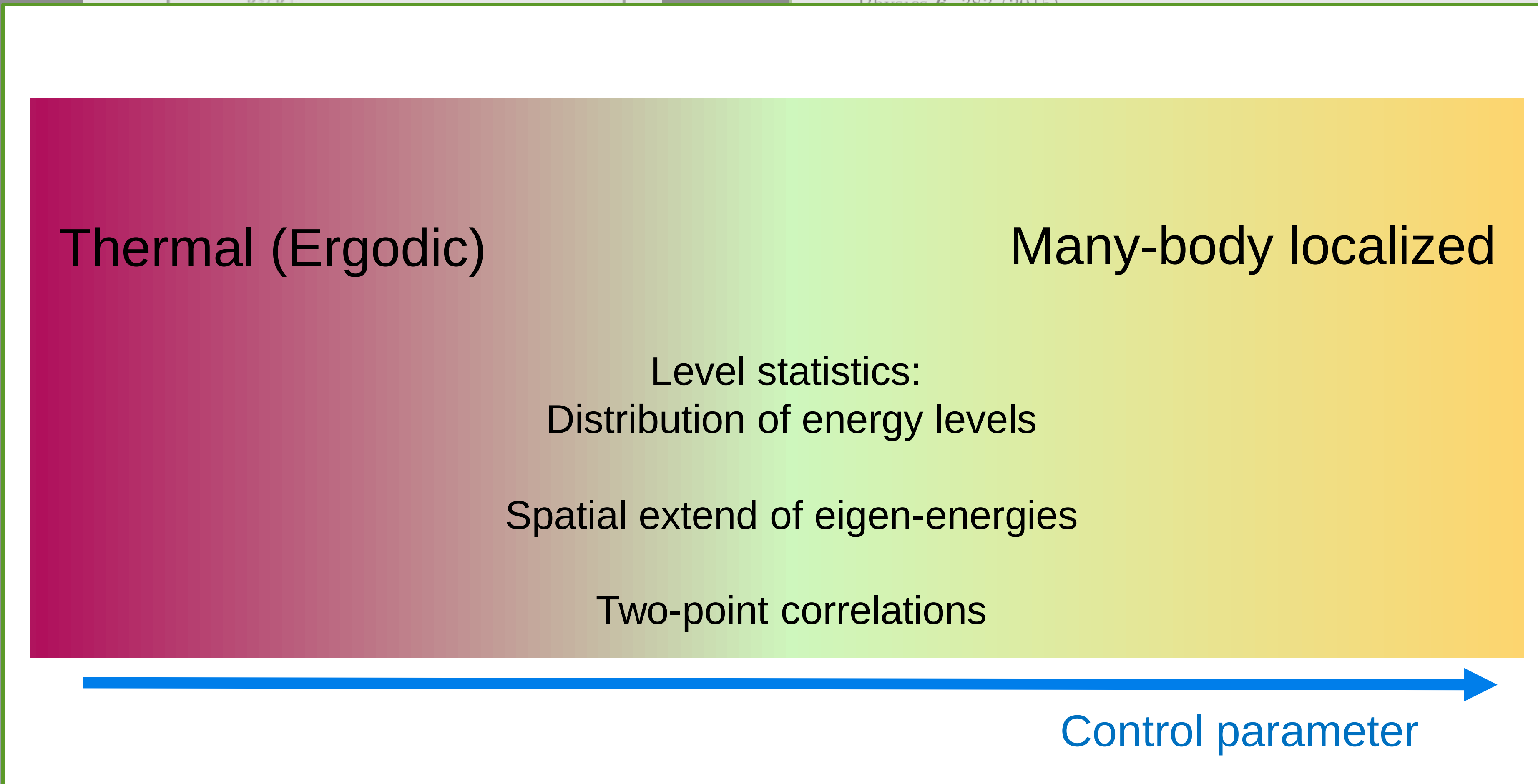

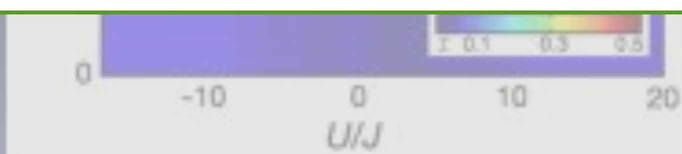

Nature Communications **6**, 7341 (2015).
[15] John Z. Imbrie, "Diagonalization and many-body localization for a disordered quantum spin chain," Phys. Rev. Lett. **117**, 027201 (2016).
[16] F. Iemini, A. Russomanno, D. Rossini, A. Scardicchio, and R. Fazio, "Signatures of many-body localization in the dynamics of two-site entanglement," Phys. Rev. B **94**, 214206 (2016).

Time-domain spectroscopy-I

$$|\psi(t)\rangle = \sum_\alpha C_\alpha e^{-iE_\alpha t/\hbar}|\phi_\alpha\rangle \quad \text{, where} \quad \hat{H}|\phi_\alpha\rangle = E_\alpha|\phi_\alpha\rangle$$

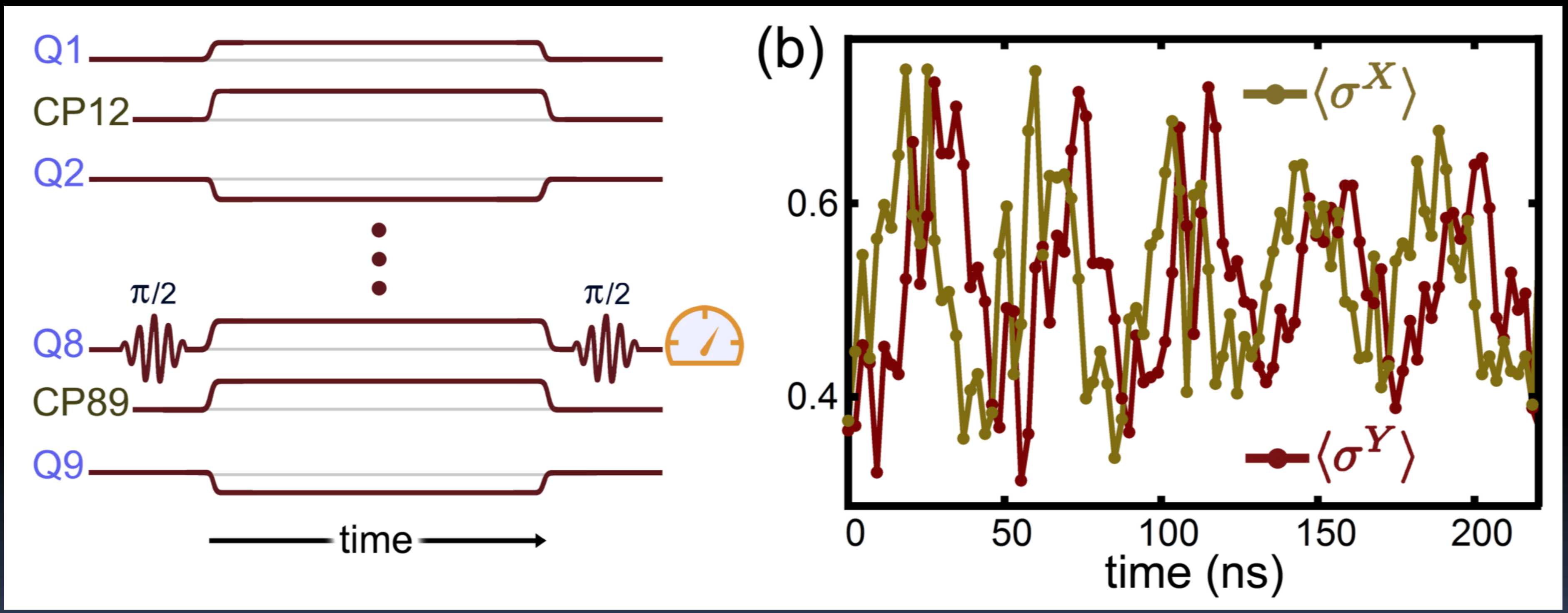

$$\hat{H} = \sum_{i=1}^{N_Q=9} h_i \sigma_i^Z + J \sum \sigma_i^X \sigma_{i+1}^X + \sigma_i^Y \sigma_{i+1}^Y$$

Roushan *et al.*, Science (2017)

Time-domain spectroscopy-II

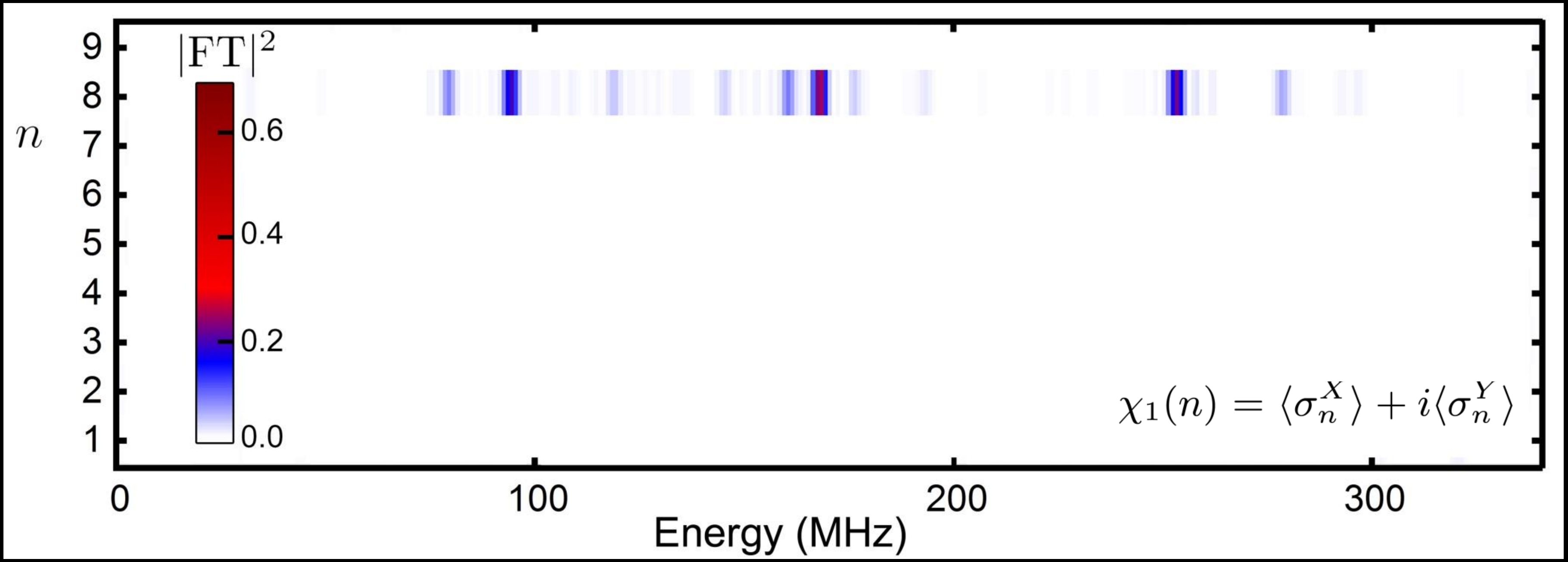

Time-domain spectroscopy-II

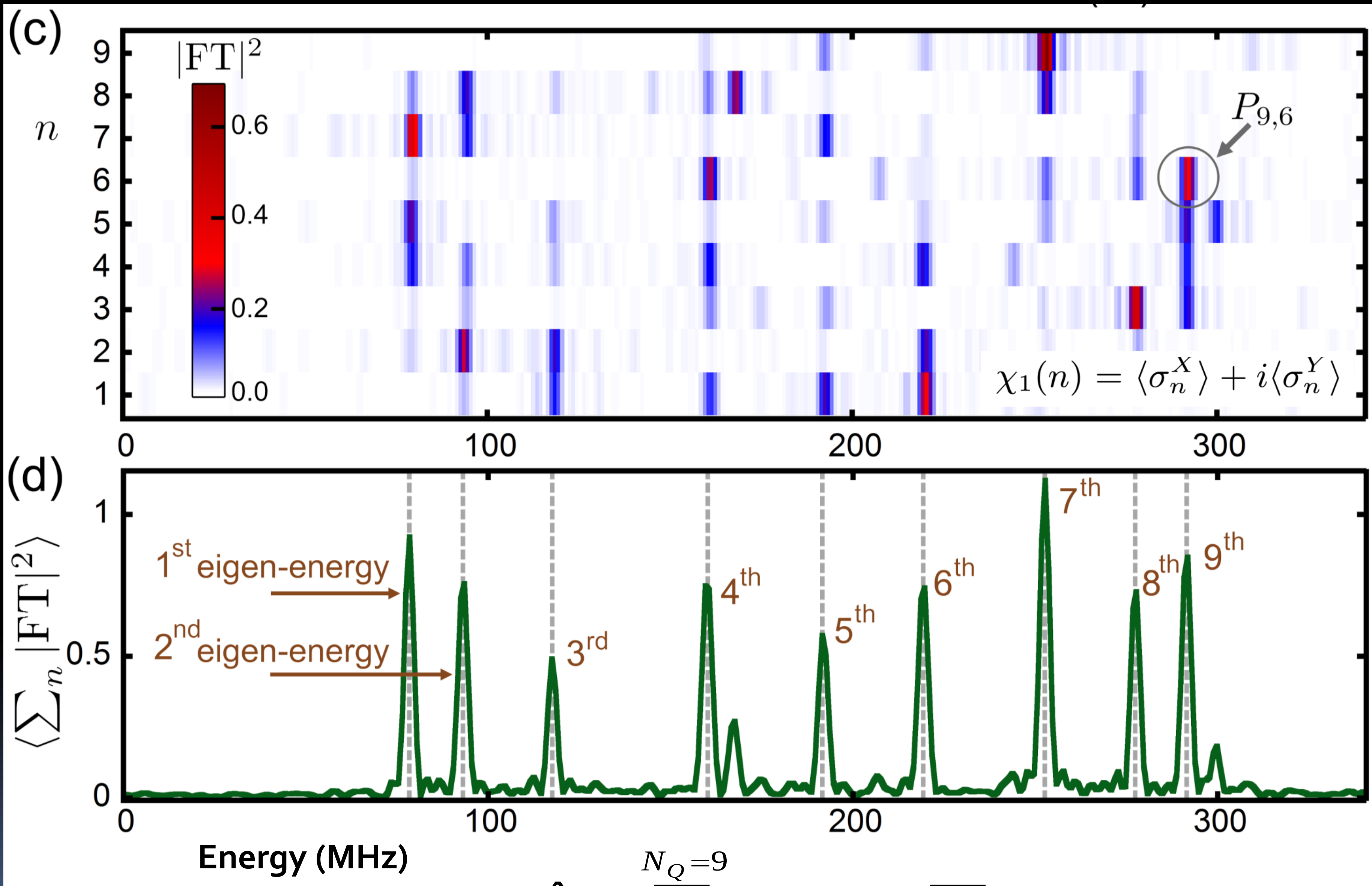

$$\hat{H} = \sum_{i=1}^{N_Q=9} h_i \sigma_i^Z + J \sum \sigma_i^X \sigma_{i+1}^X + \sigma_i^Y \sigma_{i+1}^Y$$

Time-domain spectroscopy

In our method:

$$|\psi(t)\rangle = \sum_{\alpha} C_\alpha e^{-iE_\alpha t}|\phi_\alpha\rangle$$

We measure observables:

$$\hat{O} = \sum_{\alpha,\alpha'} O_{\alpha',\alpha}|\phi_{\alpha'}\rangle\langle\phi_\alpha|$$

, where

$$O_{\alpha',\alpha} = \langle\phi_{\alpha'}|\hat{O}|\phi_\alpha\rangle$$

Which becomes

$$O(t) = \langle\psi(t)|\hat{O}|\psi(t)\rangle = \sum_{\alpha,\alpha'} O_{\alpha',\alpha}C_\alpha C^*_{\alpha'}e^{-i(E_\alpha - E_{\alpha'})t}$$

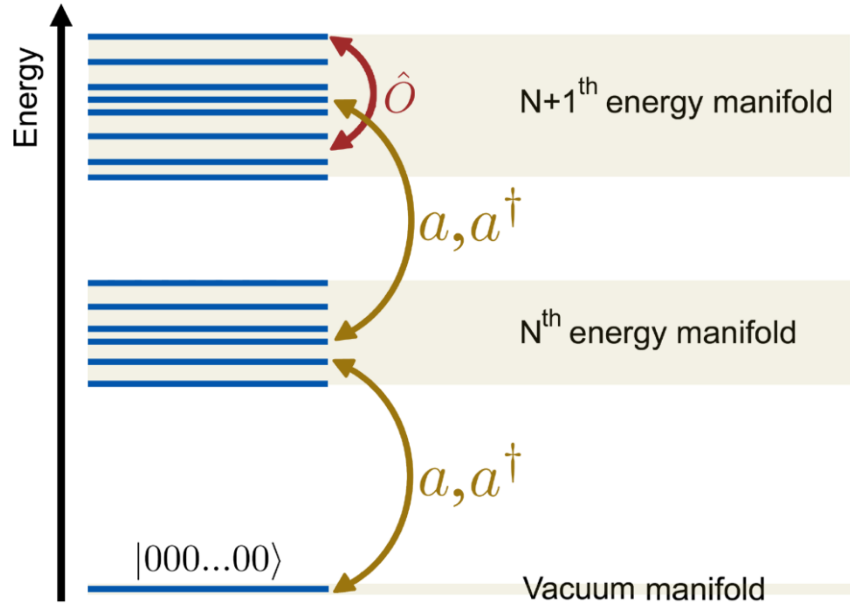

Initial states \ operators	$\langle a_1^\dagger a_1\rangle$	$\langle a_1\rangle$
$\lvert\psi_0\rangle = \lvert 10\rangle$	$\frac{1}{2}[1+\cos((E_+ - E_-)t)]$ ✗	0 ✗
$\lvert\psi_0\rangle = \frac{\lvert 00\rangle + \lvert 10\rangle}{\sqrt{2}}$	$\frac{1}{4}[3+\cos((E_+ - E_-)t)]$ ✗	$\frac{1}{4}\left(e^{-iE_+t} + e^{-iE_-t}\right)$ ✓

Roushan *et al.*, Science (2017)

Eigenvalues of 1D Harper model

$$\hat{H}(b) = \Delta \sum_{i=1}^{N_Q=9} \cos(2\pi n b)\sigma_i^Z + \sum J_i(\sigma_i^X \sigma_{i+1}^X + \sigma_i^Y \sigma_{i+1}^Y)$$

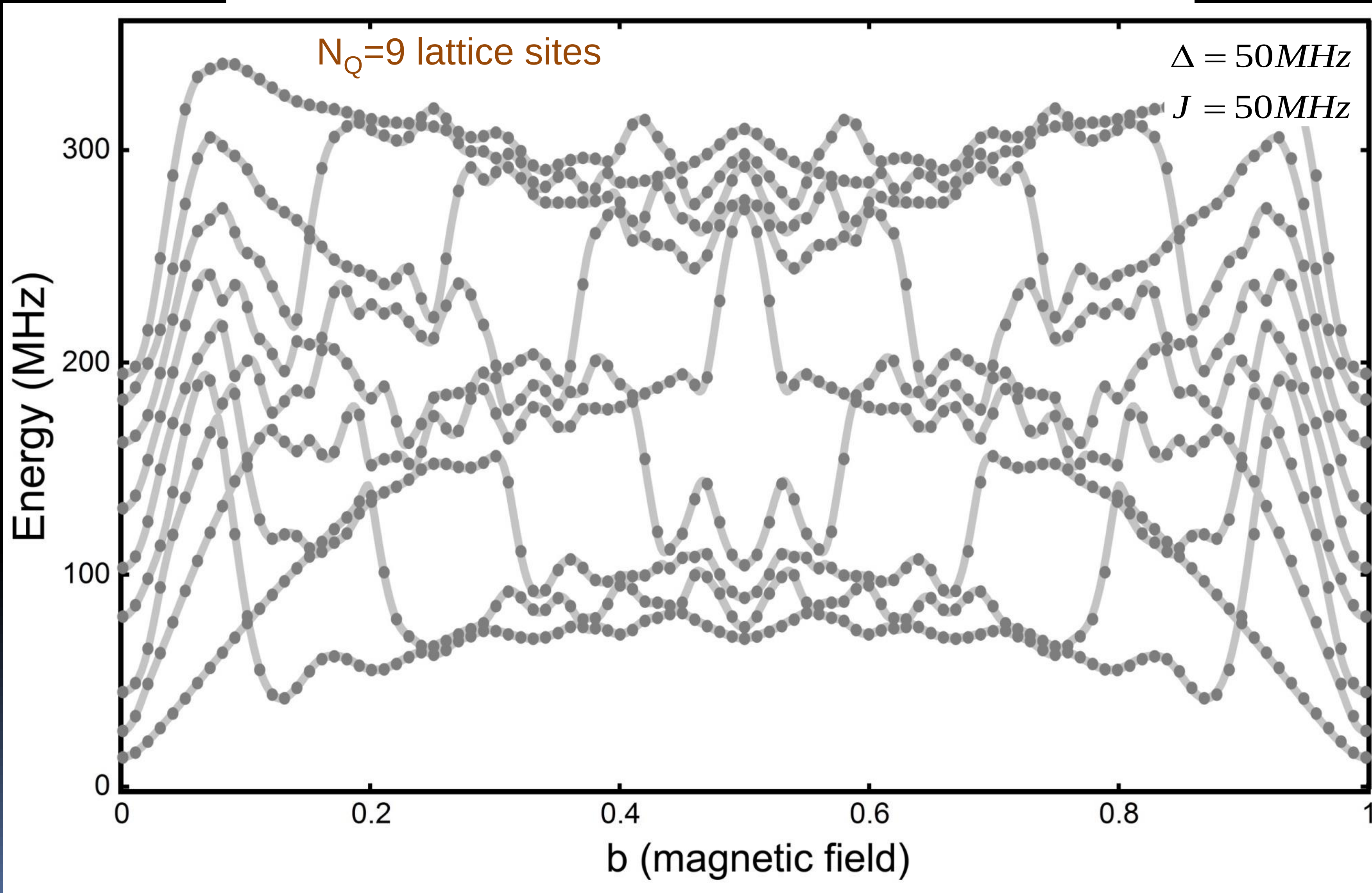

9 qubit Hofstadter Butterfly

$$\hat{H}(b) = \Delta \sum_{i=1}^{N_Q=9} \cos(2\pi n b)\sigma_i^Z + \sum J_i(\sigma_i^X \sigma_{i+1}^X + \sigma_i^Y \sigma_{i+1}^Y)$$

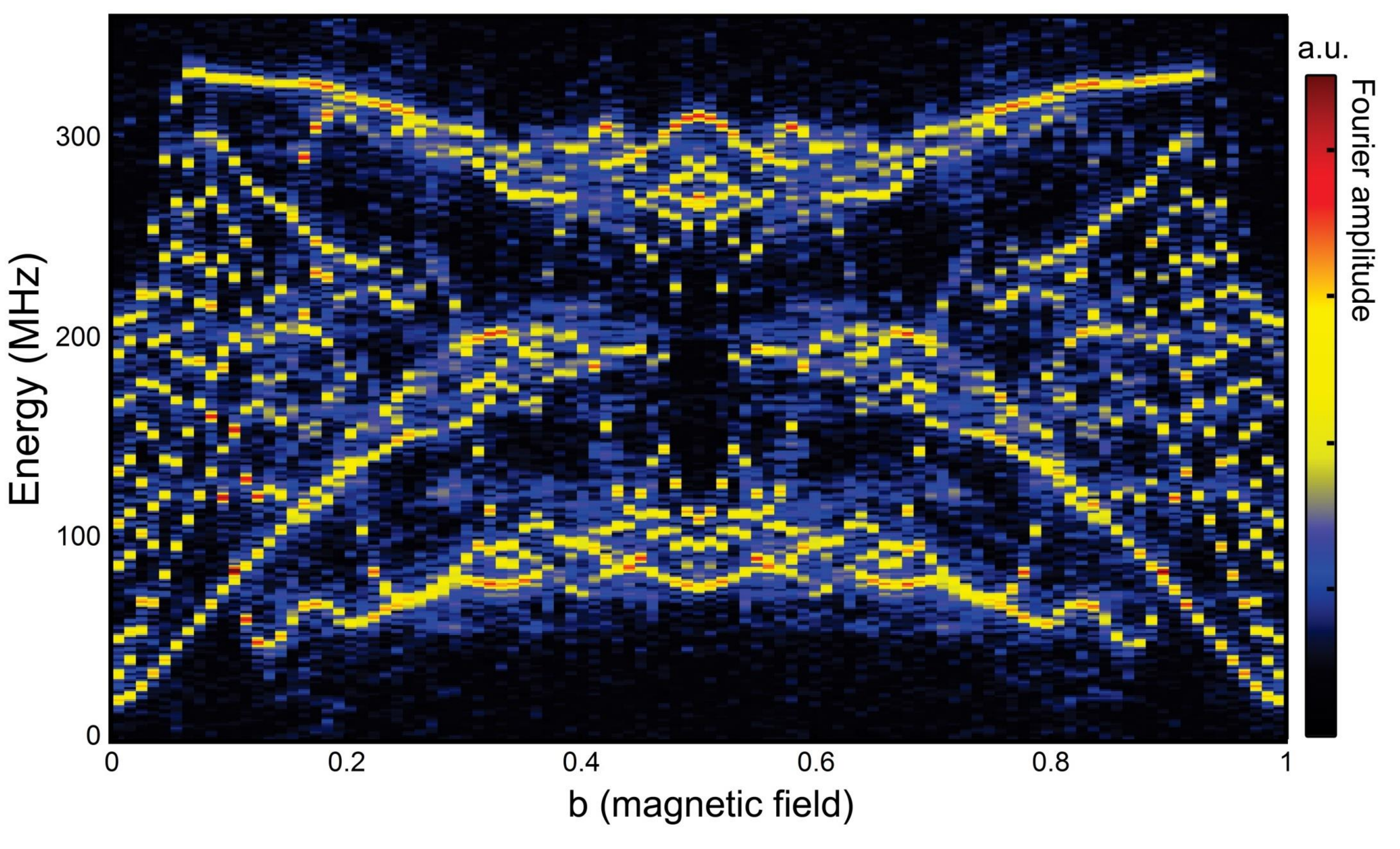

9 qubit Hofstadter Butterfly

$$\hat{H}(b) = \Delta \sum_{i=1}^{N_Q=9} \cos(2\pi n b)\sigma_i^Z + \sum J_i(\sigma_i^X \sigma_{i+1}^X + \sigma_i^Y \sigma_{i+1}^Y)$$

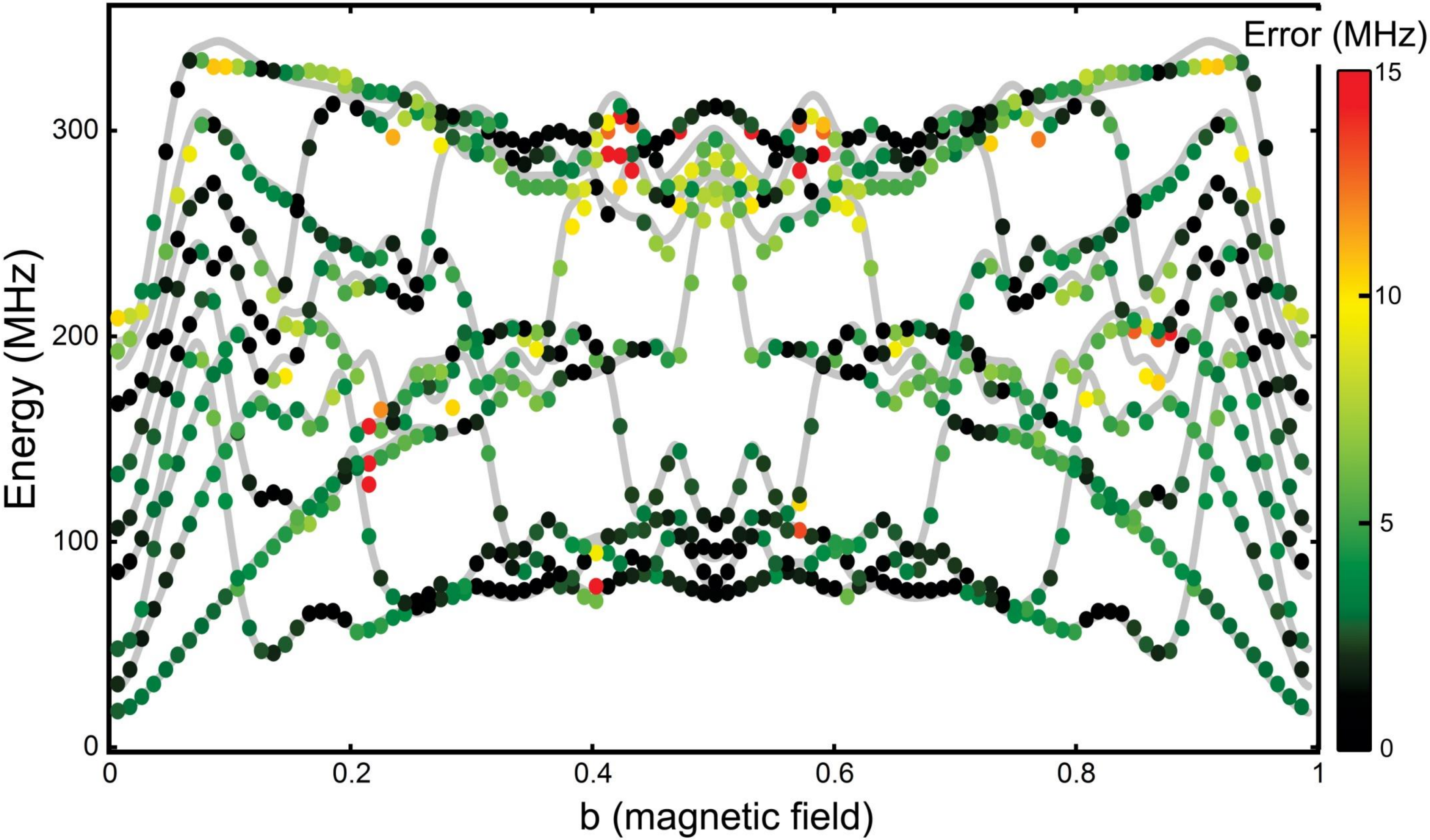

Two photons: interacting systems

$$H_{BH} = \Delta \sum_{n=1}^{9} \cos(2\pi n b) a_n^\dagger a_n + \frac{U}{2} \sum_{n=1}^{9} a_n^\dagger a_n (a_n^\dagger a_n - 1) + J \sum_{n=1}^{8} a_{n+1}^\dagger a_n + a_n^\dagger a_{n+1}$$

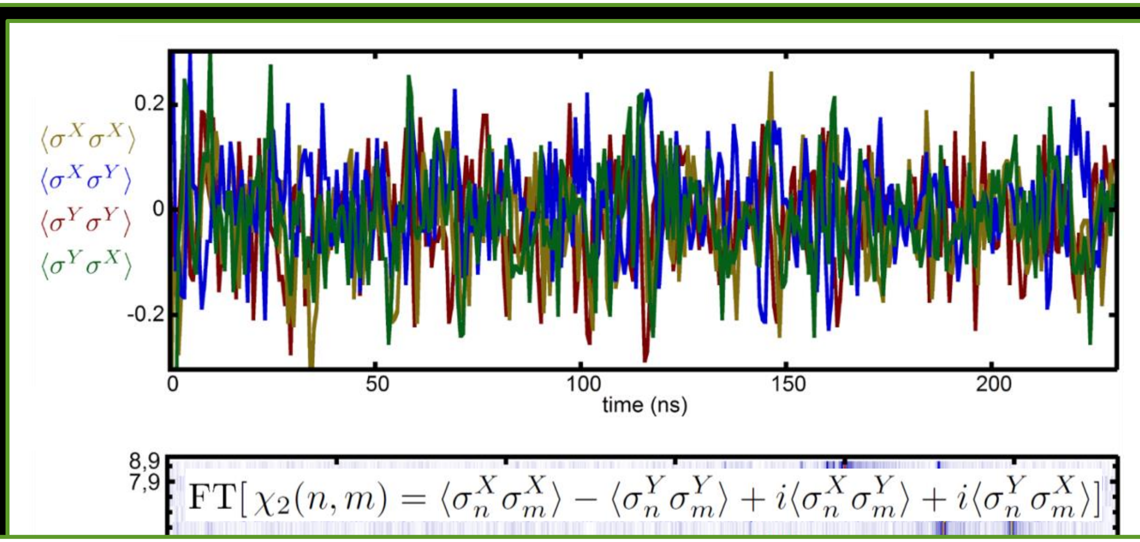

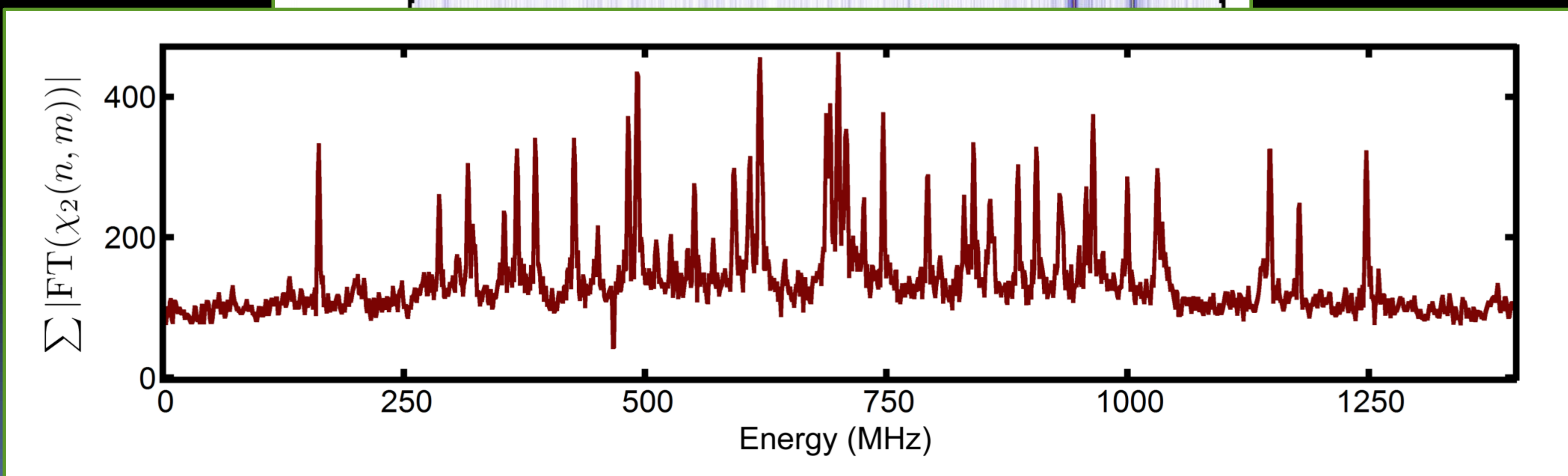

Energy level statistics

$$H_{BH} = \Delta \sum_{n=1}^{9} \cos(2\pi n b) a_n^\dagger a_n + \frac{U}{2} \sum_{n=1}^{9} a_n^\dagger a_n (a_n^\dagger a_n - 1) + J \sum_{n=1}^{8} a_{n+1}^\dagger a_n + a_n^\dagger a_{n+1}$$

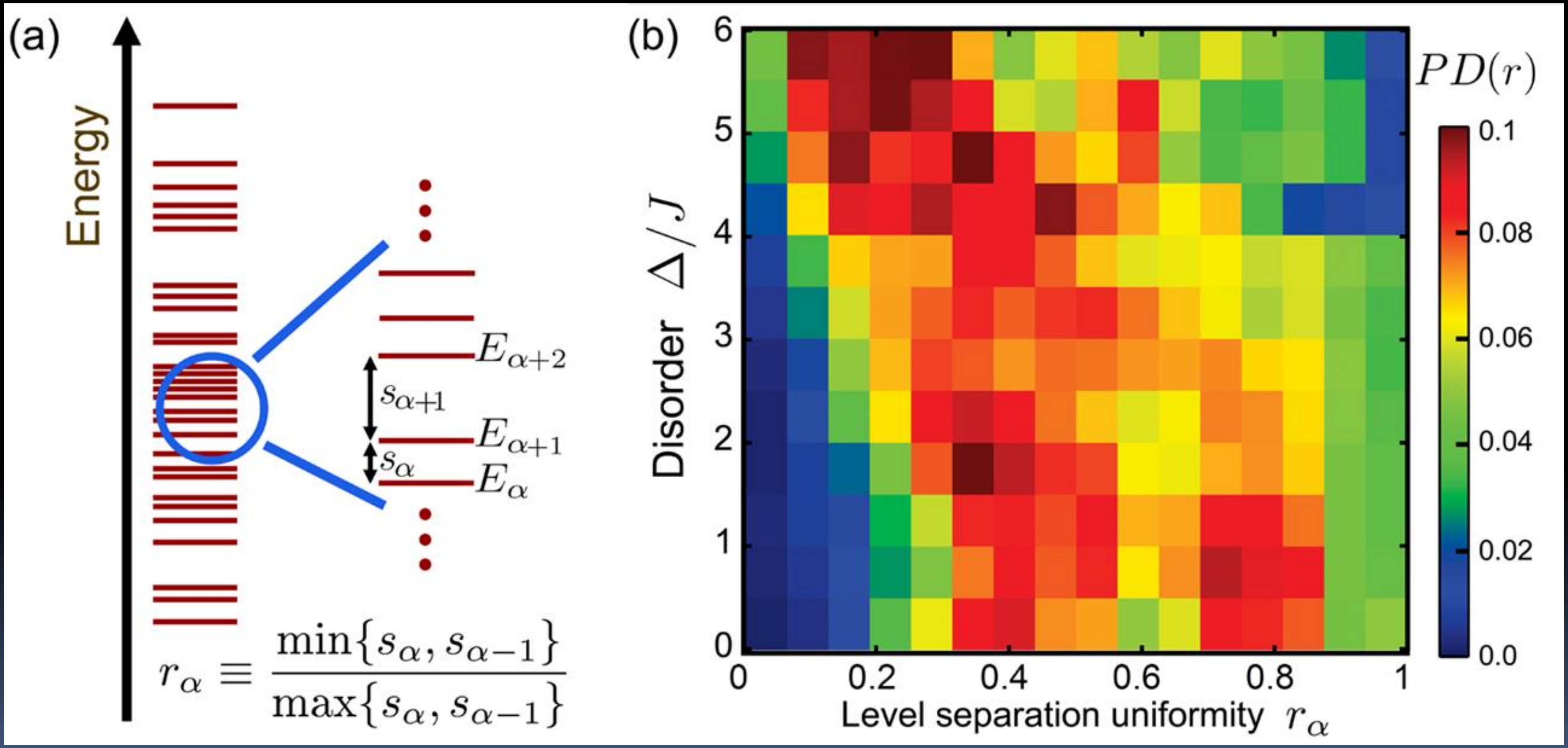

V. Oganesyan and D. Huse, PRB (2007)
Y.Y. Atas *et al.*, PRL (2013)
O. Bohigas *et al.*, PRL (1984)

Energy level statistics

$$PD_{\text{GOE}}(r) = \frac{27}{4}\frac{r+r^2}{(1+r+r^2)^{5/2}} \qquad PD_{\text{Poisson}}(r) = \frac{2}{(1+r)^2}$$

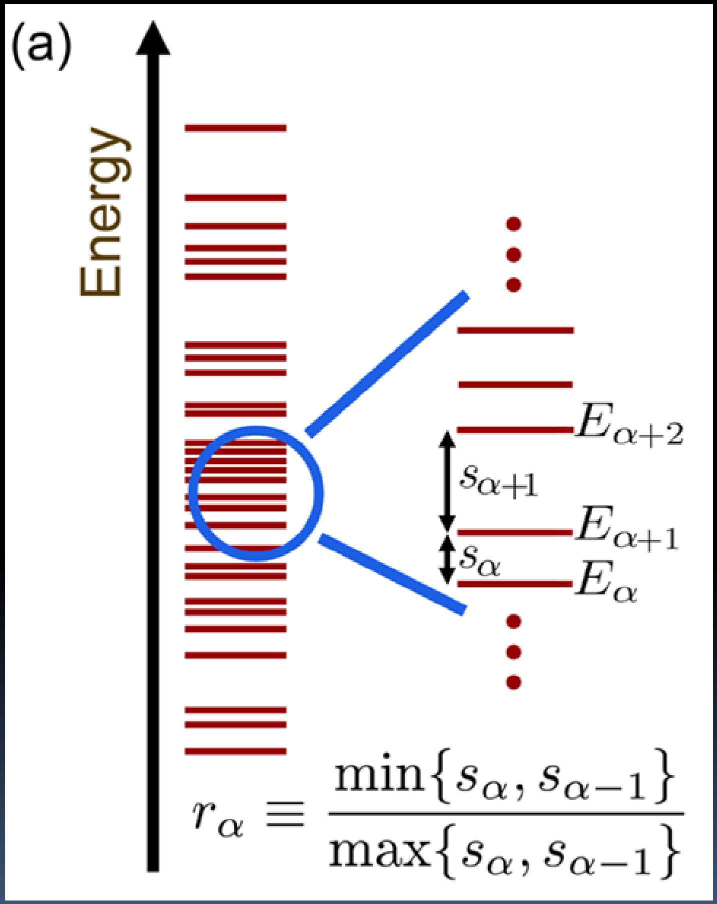

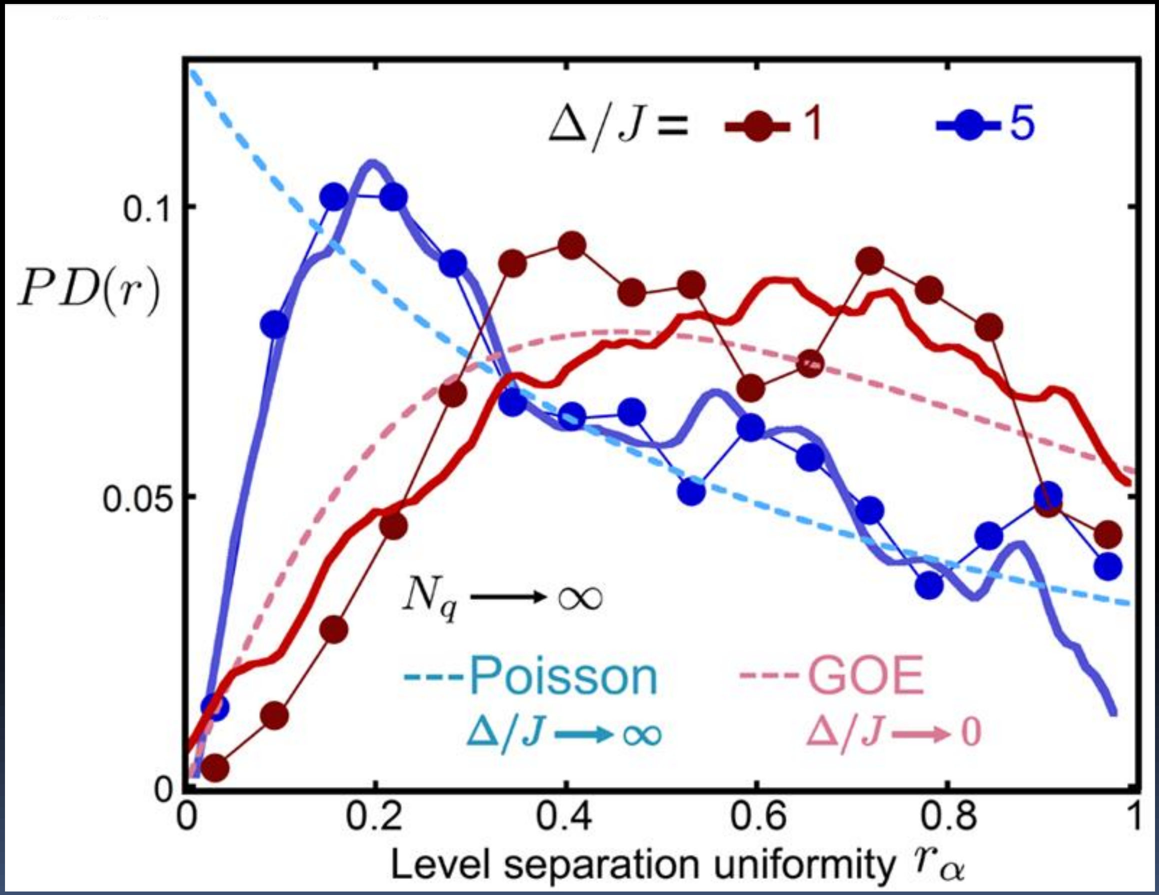

Anderson vs. Many-body localized phase

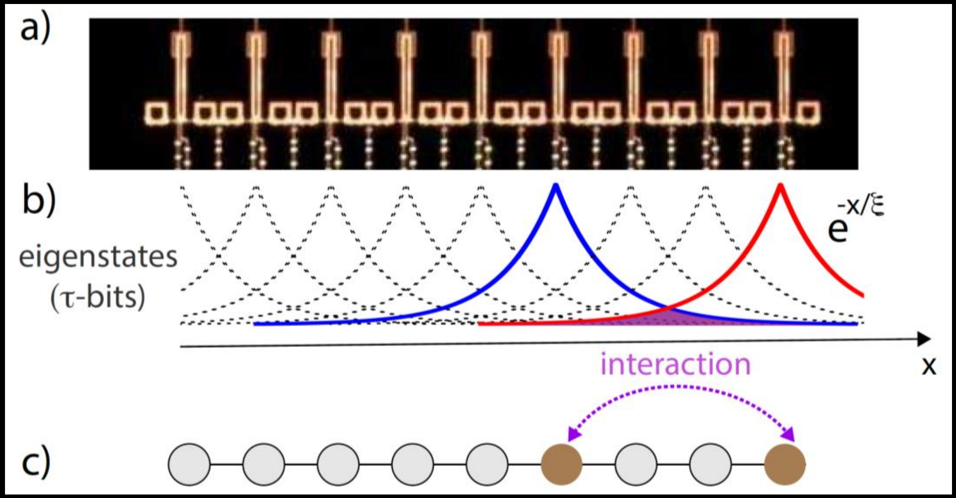

Non-interacting particles

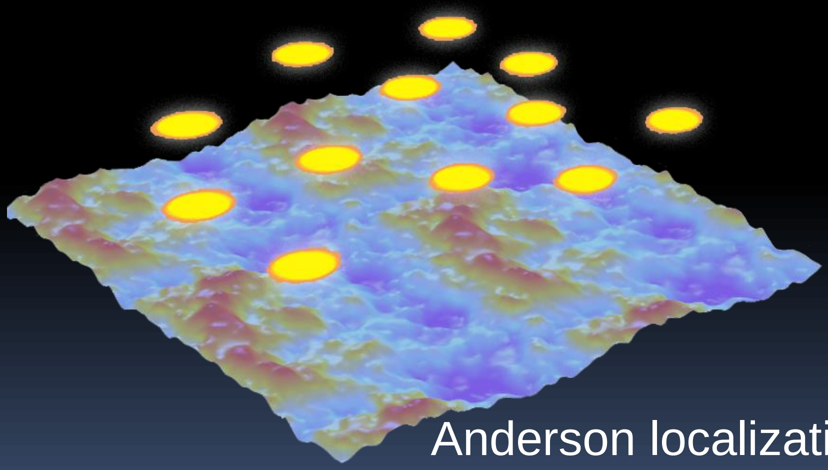

Anderson localization

Interacting particles

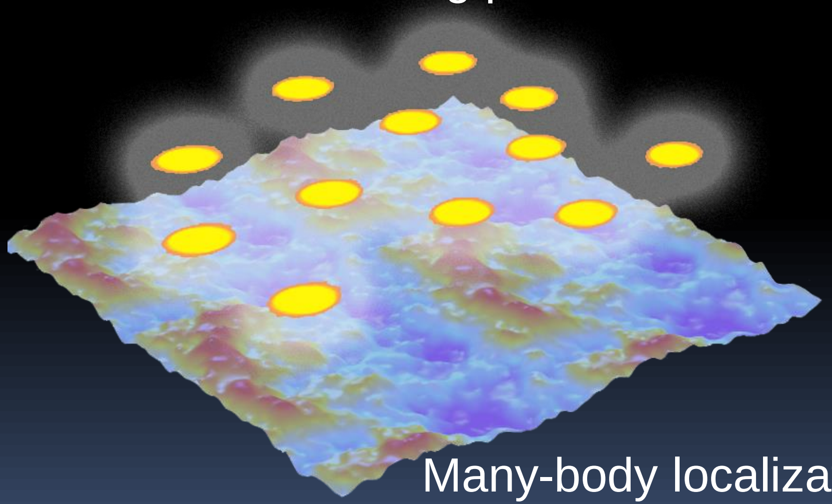

Many-body localization

P. W. Anderson (1958)
Absence of diffusion in certain random lattices

Basko, Aleiner, and Altshuler (2006)
Metal-insulator transition in a weakly interacting many-electron system with localized single-particle states

$$\hat{H}_{BH} = \sum_{i=1}^{N_Q=9} h_i a_i^+ a_i + \frac{U}{2}\sum_i n_i(n_i-1) + g\sum a_i^+ a_{i+1} + a_{i+1}^+ a_i$$

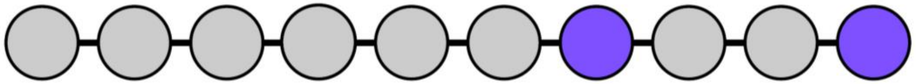

$$h_i \in [-W, W]$$

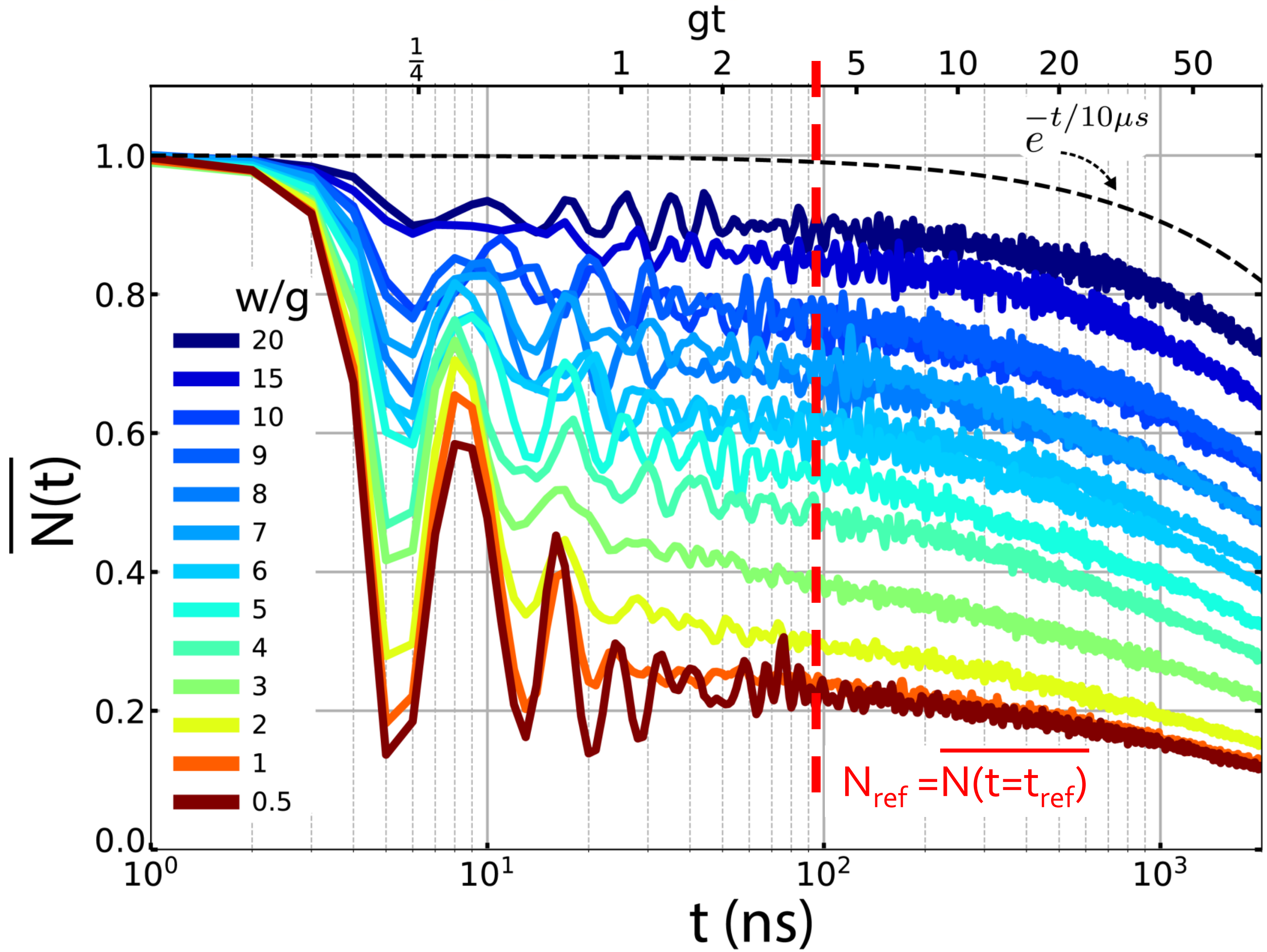

Breakdown of Ergodicity

$$\hat{H}_{BH} = \sum_{i=1}^{N_Q=9} h_i a_i^+ a_i + \frac{U}{2}\sum_i n_i(n_i - 1) + g\sum a_i^+ a_{i+1} + a_{i+1}^+ a_i$$

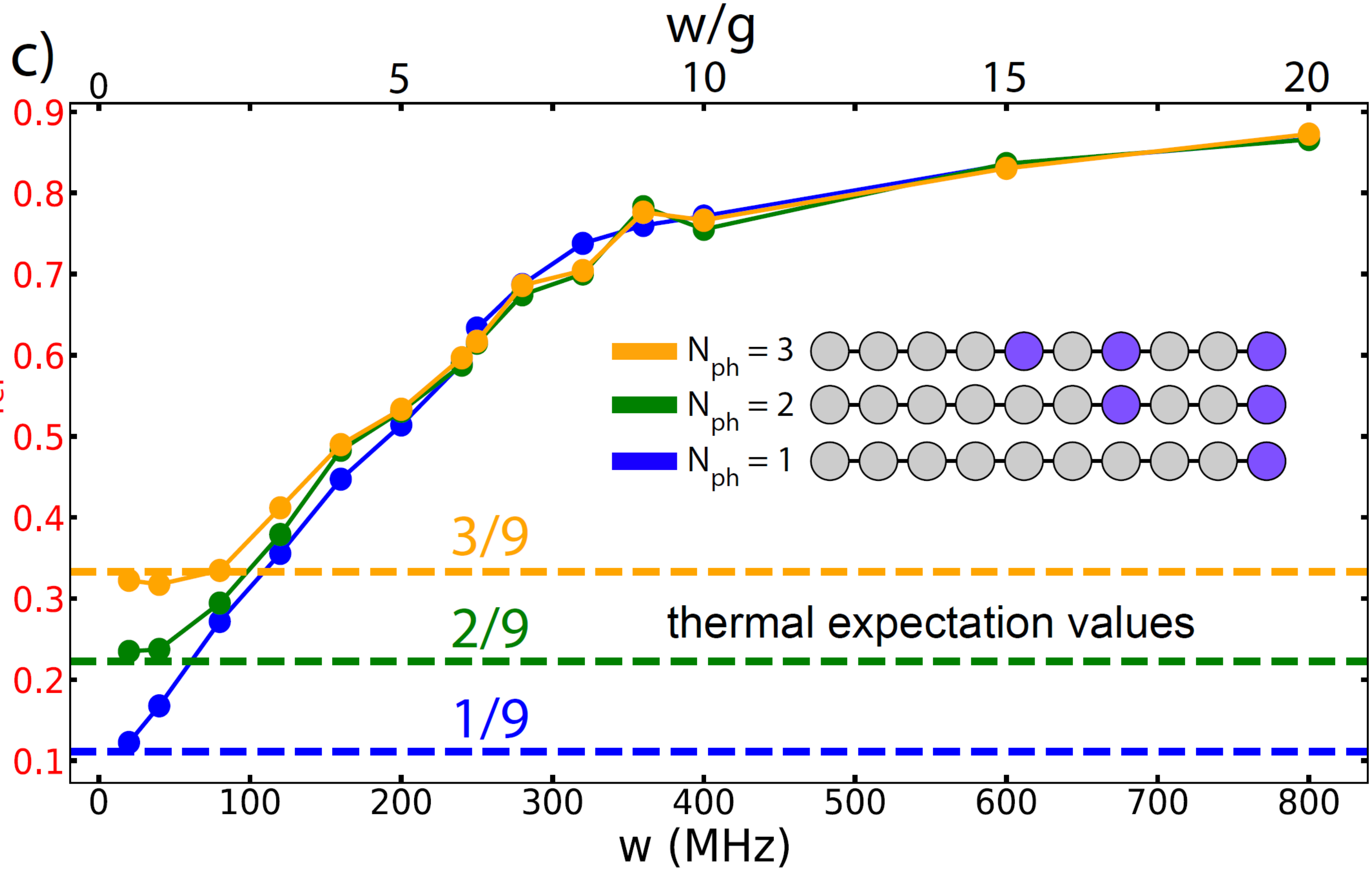

Histograms: mean and standard deviation

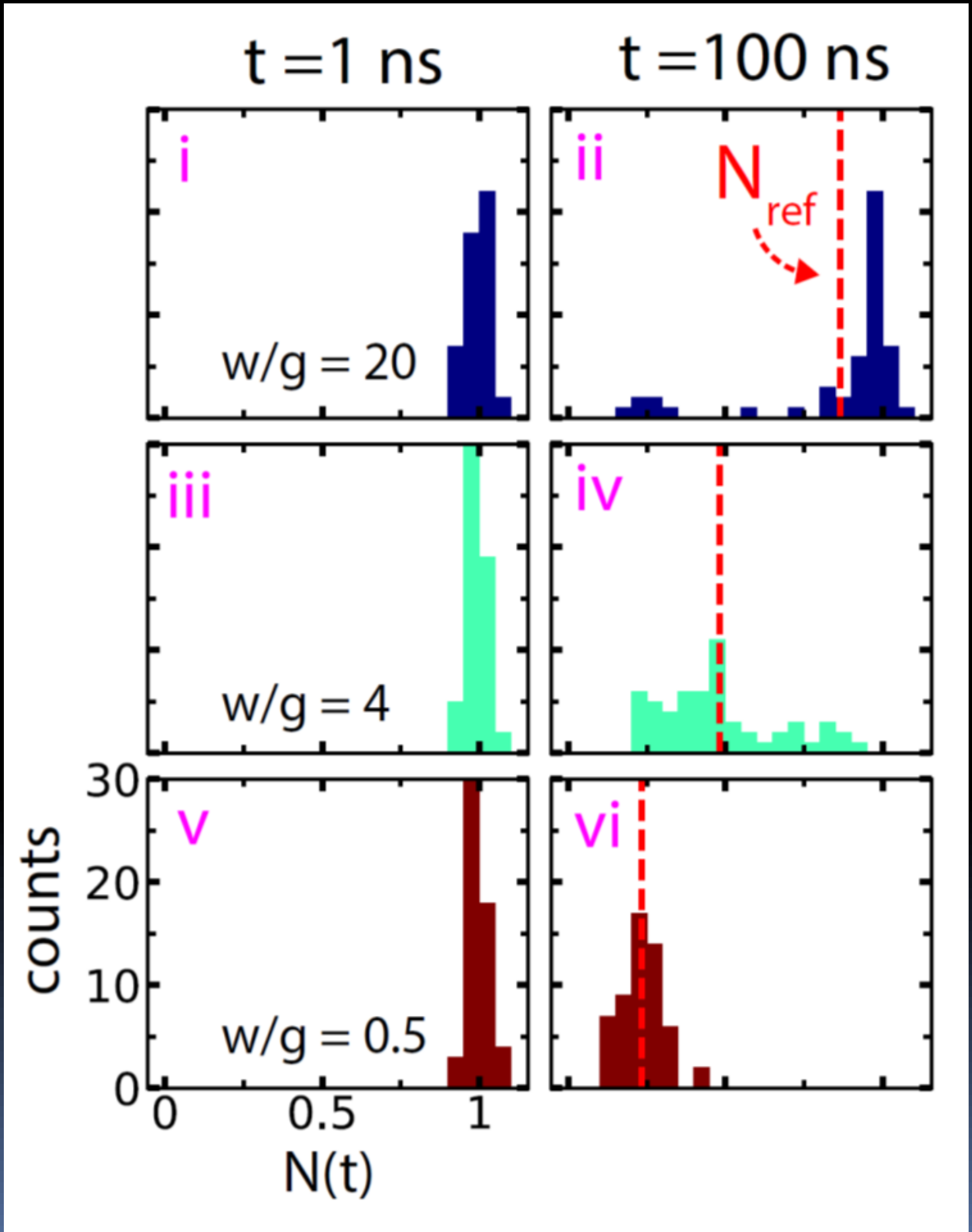

Damping of fluctuations in the MBL phase

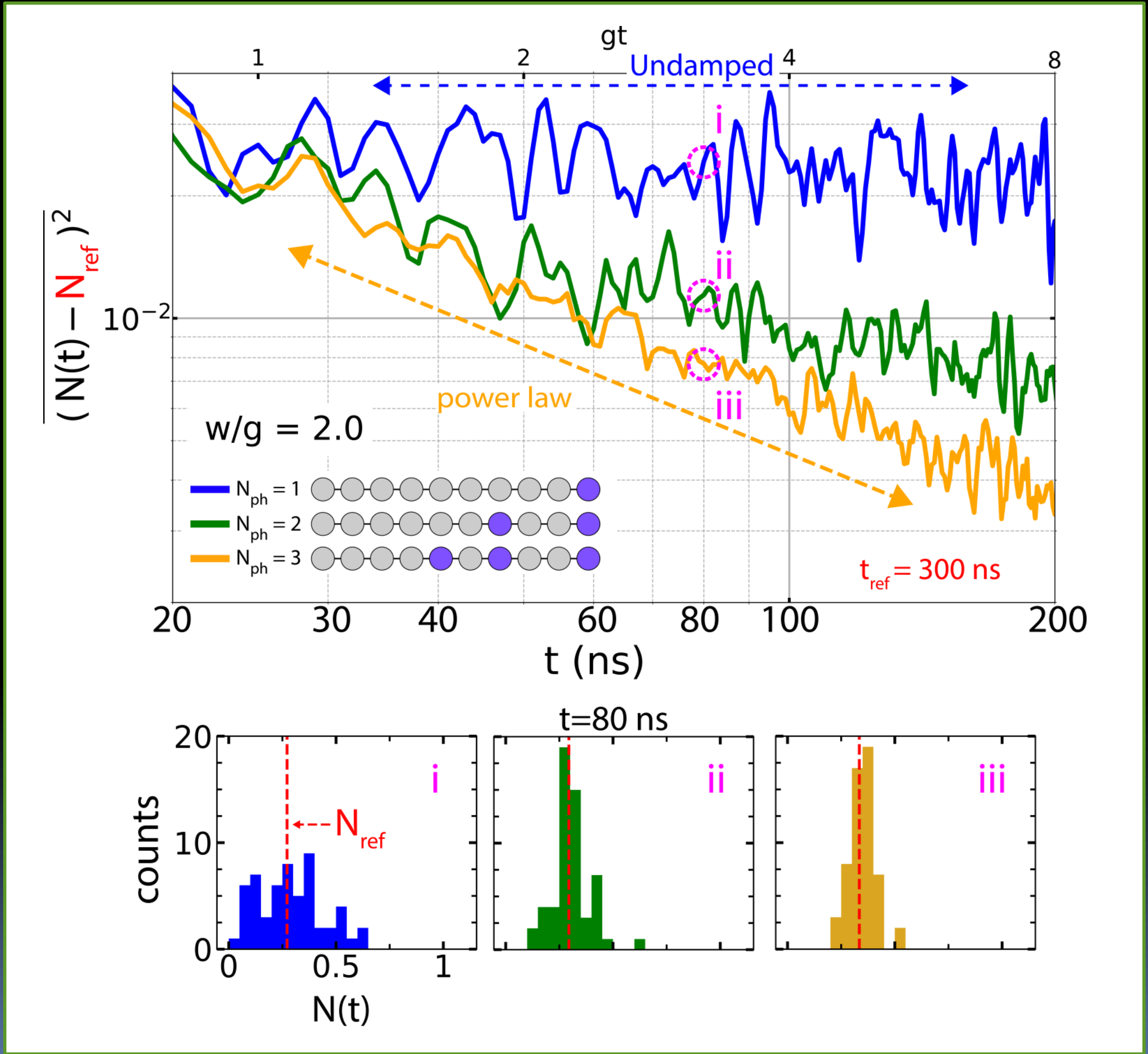

Evolution of 2-qubit reduced density matrix

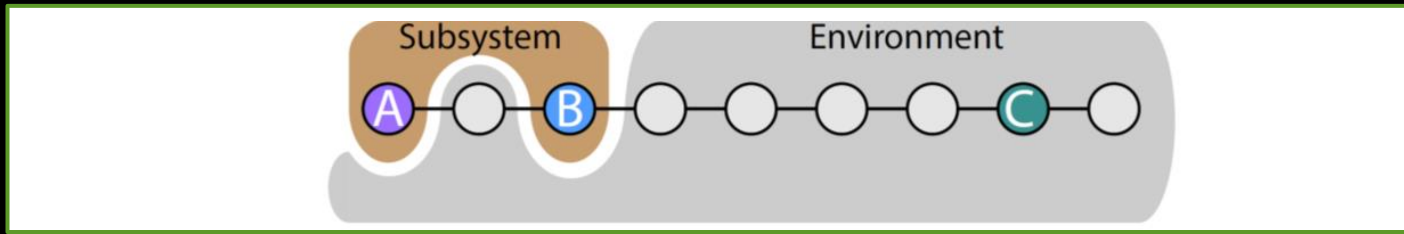

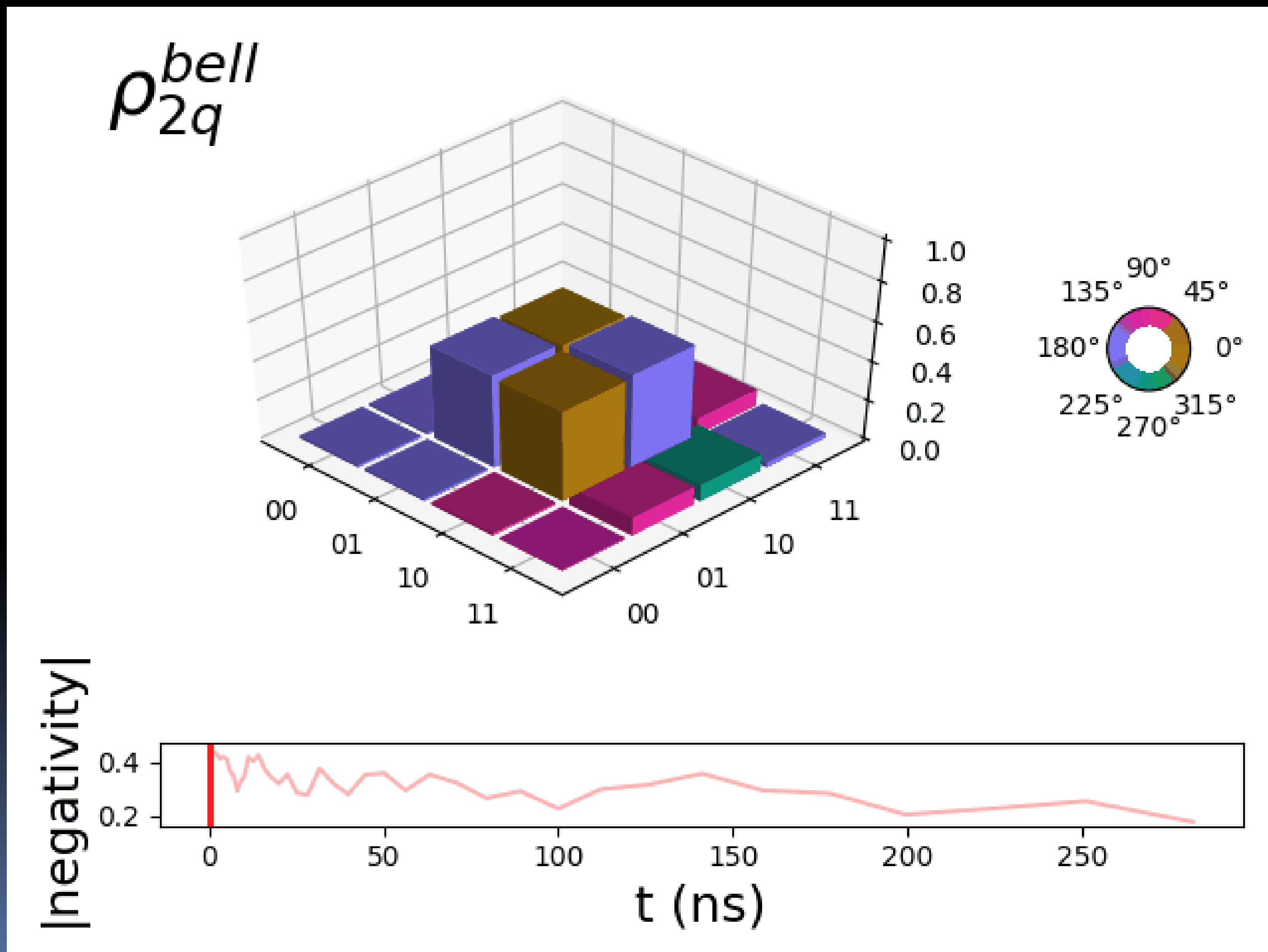

Repetition rate 20KHz

Logarithmic growth of entanglement

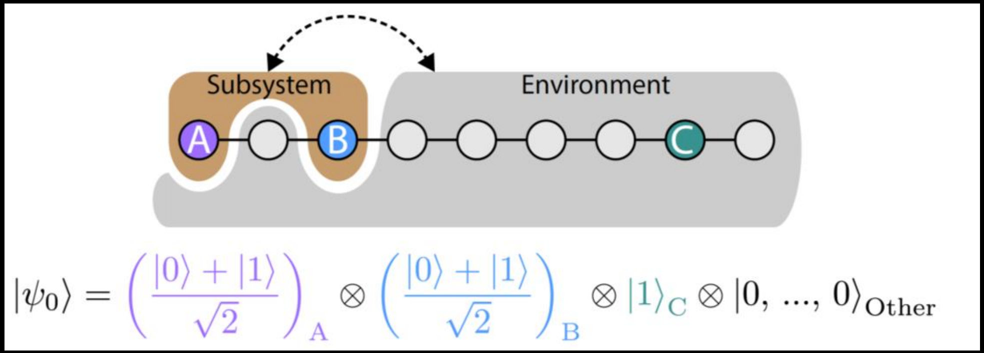

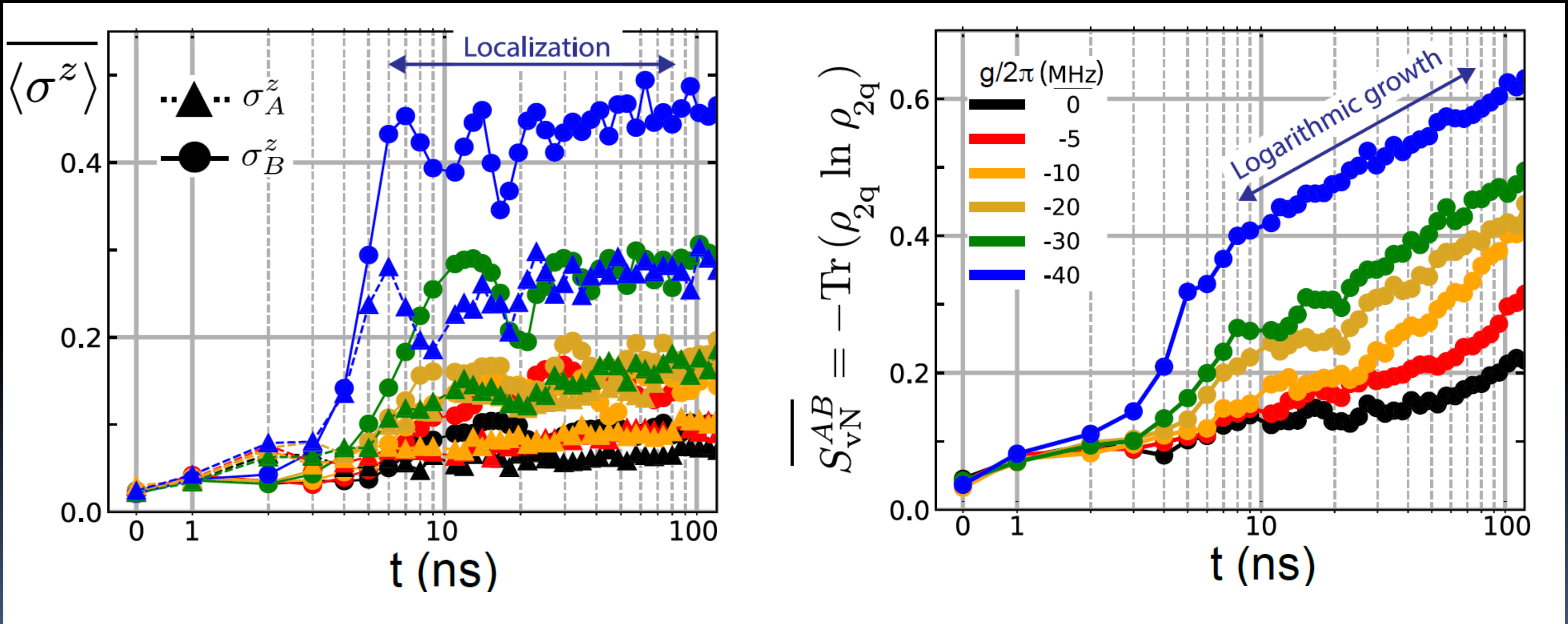

Growth and preservation of Entangle…

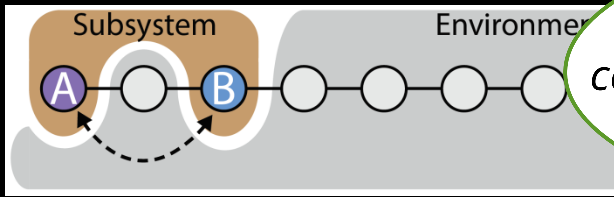

Yes ! believe me. It needs to be complicated. It is a job security kind of thing…

Michael Knap

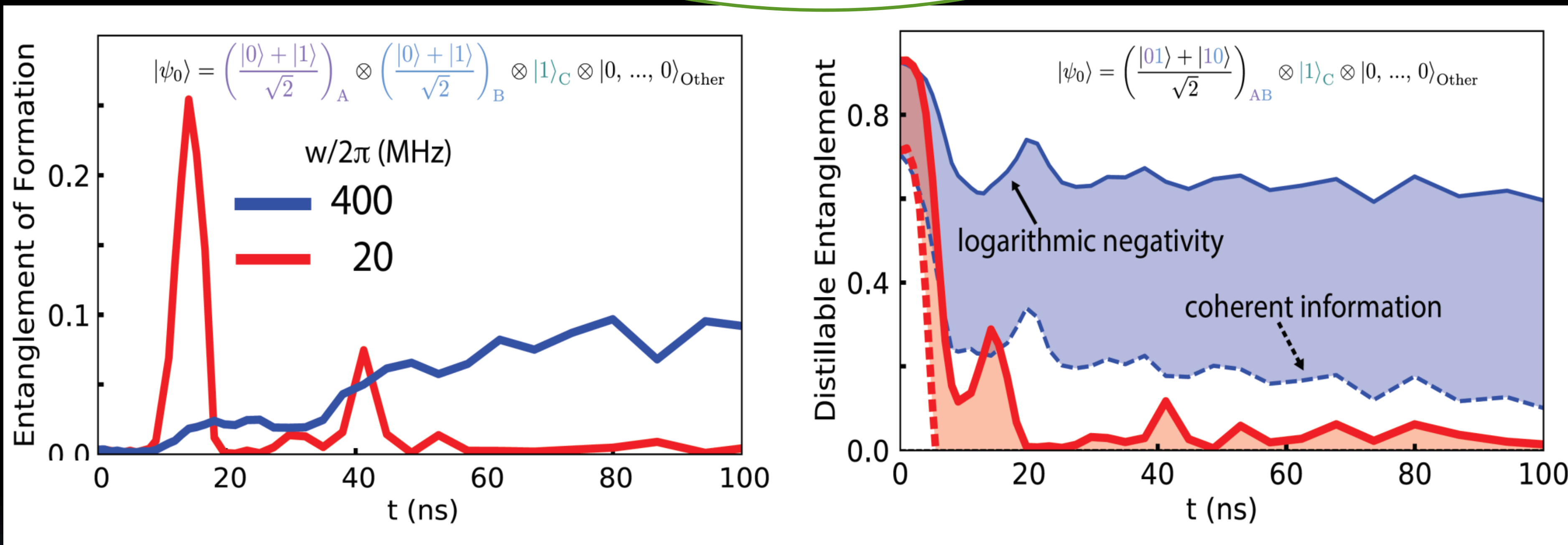

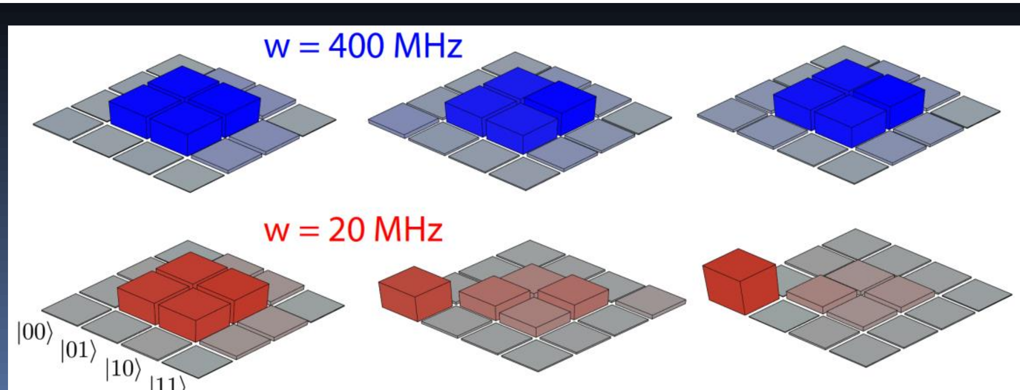

Participation ratio

We are interested in:

$$|\phi_\alpha\rangle = \sum_n C_{\alpha,n} |\mathbf{1}_n\rangle$$

Our method:

$$|\psi(t)\rangle = \sum_\alpha C_\alpha e^{-iE_\alpha t/\hbar} |\phi_\alpha\rangle$$

At time=0:

$$|\psi_0\rangle = \sum_\alpha C_\alpha |\phi_\alpha\rangle$$

Fock state as initial state:

$$|\mathbf{1}_n\rangle = \sum_\alpha C_{n,\alpha} |\phi_\alpha\rangle$$

$$P_{\alpha,n} = |C_{\alpha,n}|^2$$

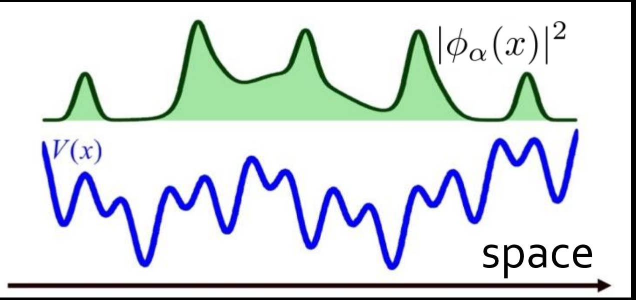

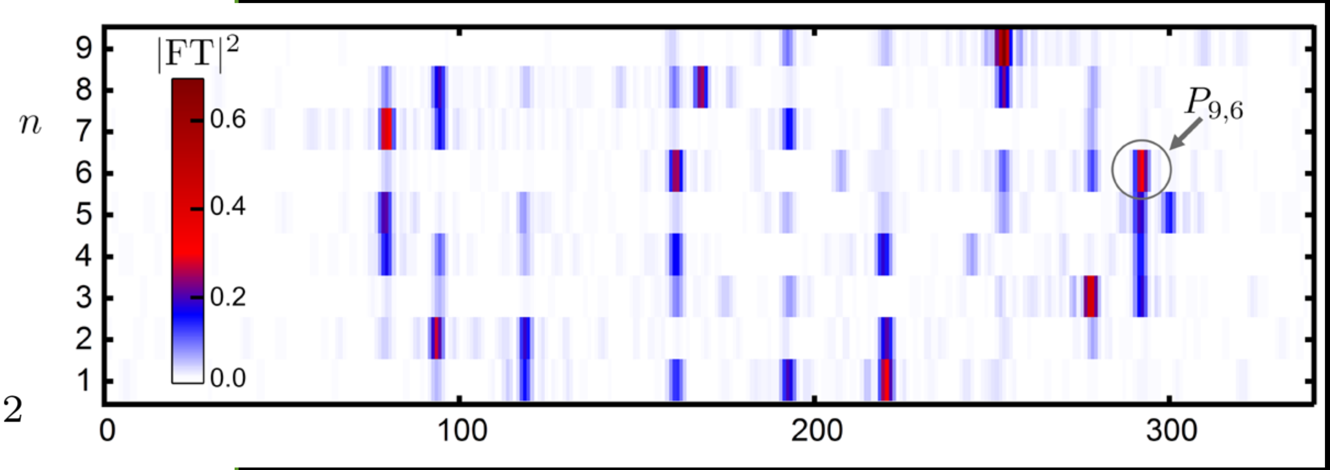

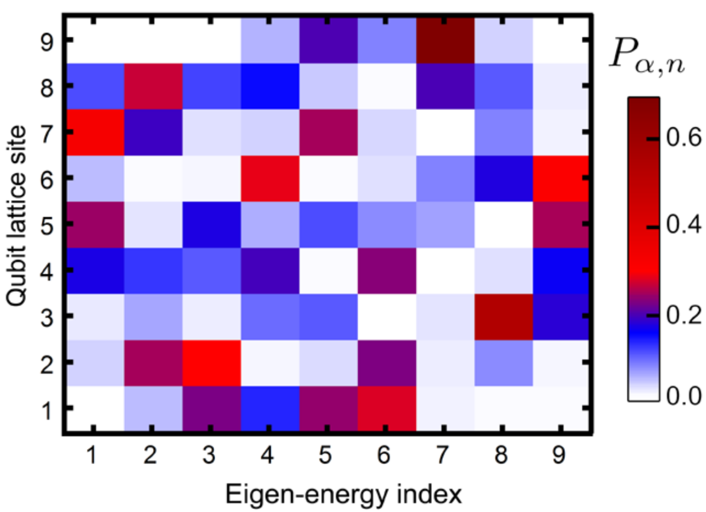

$$PR_{\text{Space}}(\alpha) \equiv 1/\sum P^2_{\alpha,n}$$

Number of energy eigenstates present in a lattice site.

$$PR_{\text{Energy}}(n) \equiv 1/\sum P^2_{\alpha,n}$$

Number of sites that an energy eigenstate is extended over.

Participation ratio

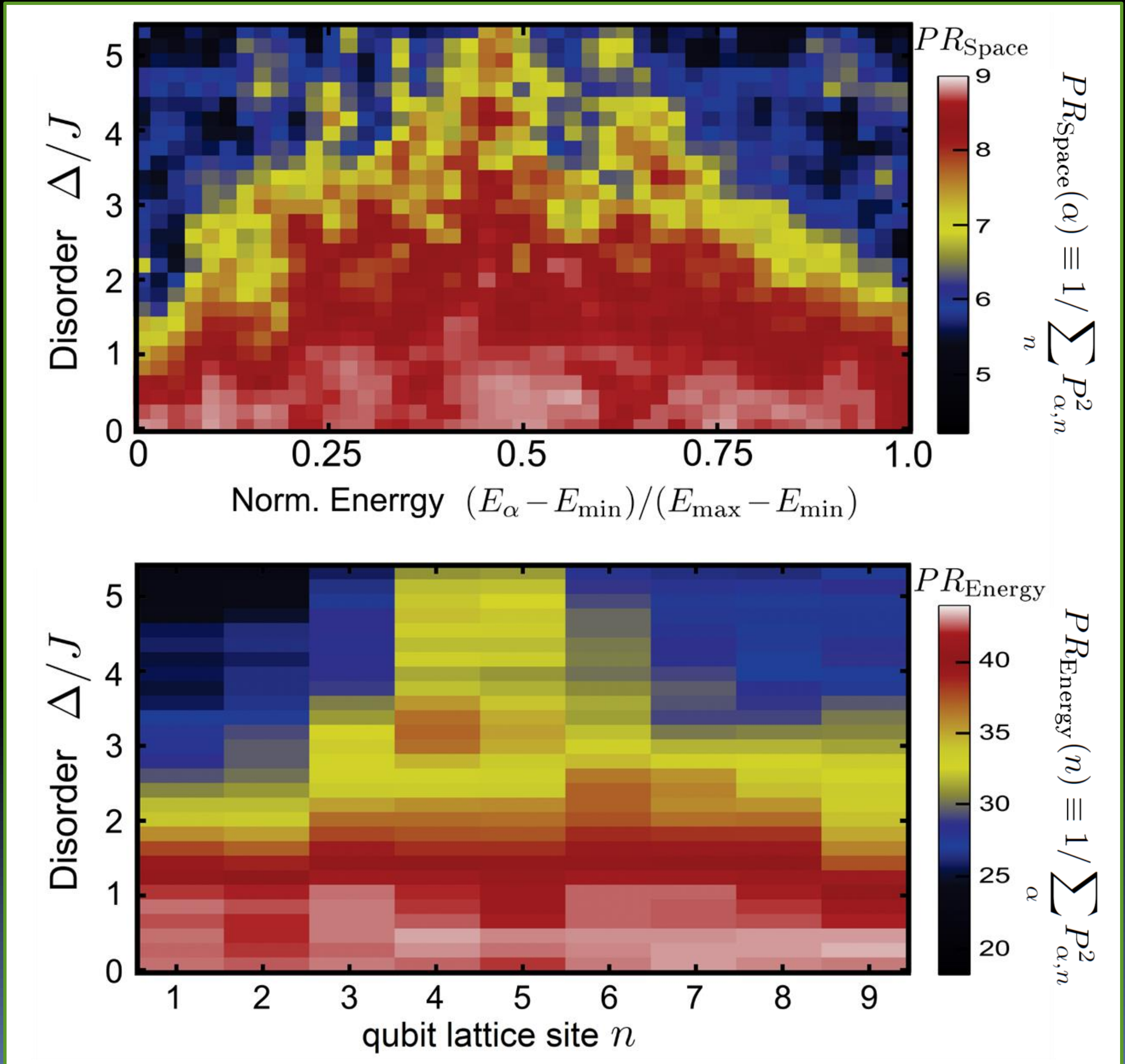

Google

Spectral signatures of MBL:

Ben Chiaro

Charles Neill

V. Bastidas

J. Tangpanitanon

D. Angelakis

CQT Centre for Quantum Technologies

NUS National University of Singapore

Dynamics of the MBL phase:

D. Abanin

M. Filippone

M. Knap

A. Bohrdt

UNIVERSITÉ DE GENÈVE

TUM Technische Universität München

A system engineering challenge

System performance :

- Calibration
- Single qubit and 2-qubit gate performance
- Cross-talk
- Coherence
- Readout
- leakage

Bristlecone - 72 qubit device

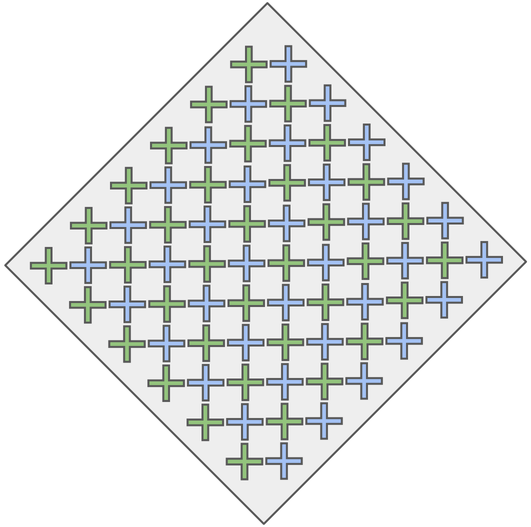

Google AI
Quantum

Single Qubit gates

Bristlecone - Single Qubit Benchmarking

Benchmark performance with random sequences of gates (RB)

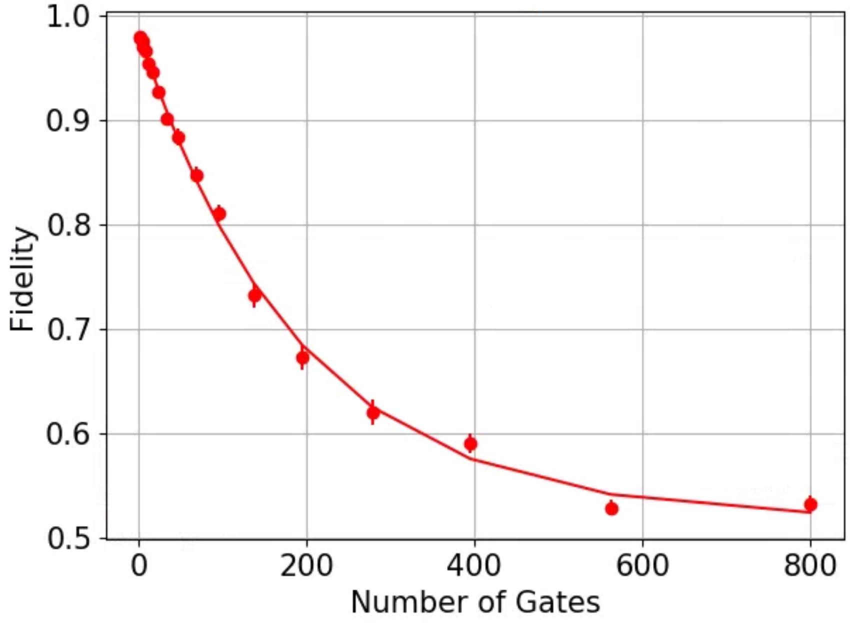

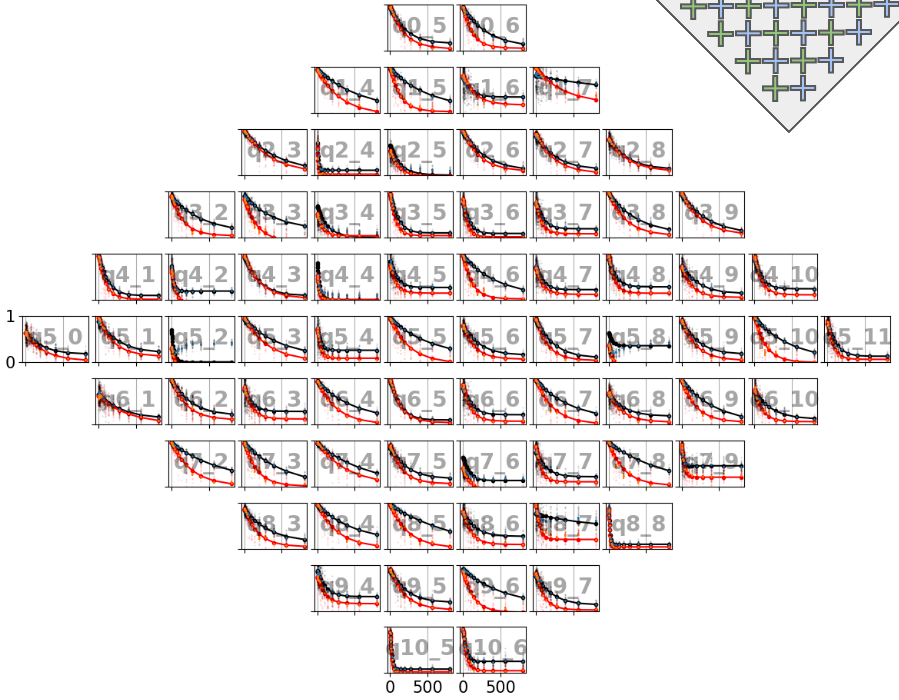

Bristlecone grid

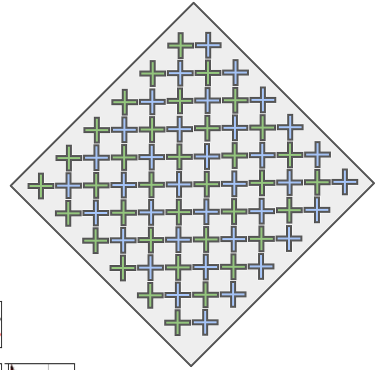

Google AI Quantum

Analysis - Heatmap

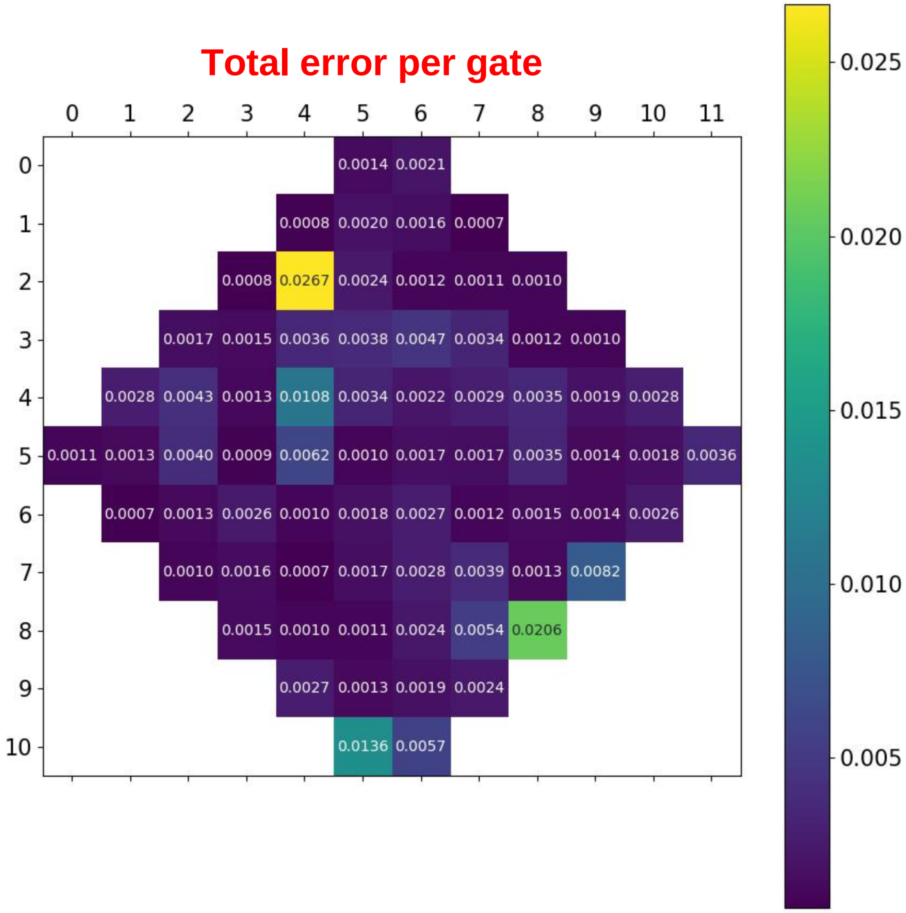

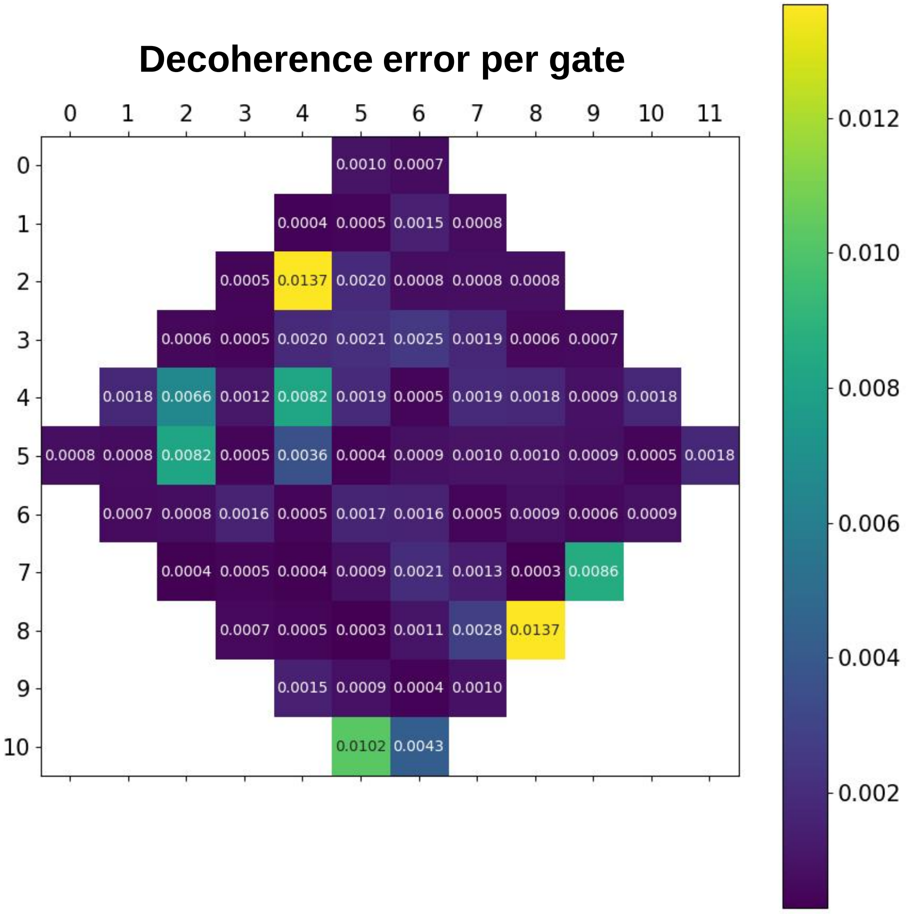

Analysis - Histogram

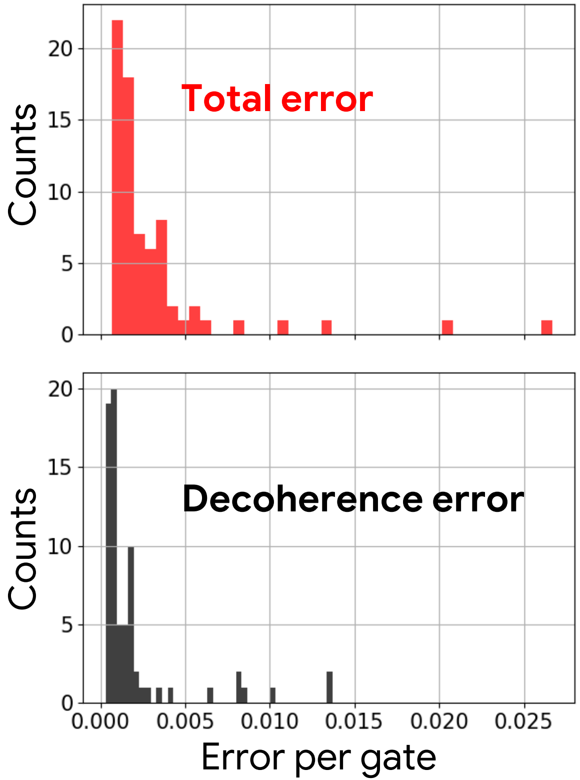

Integrate

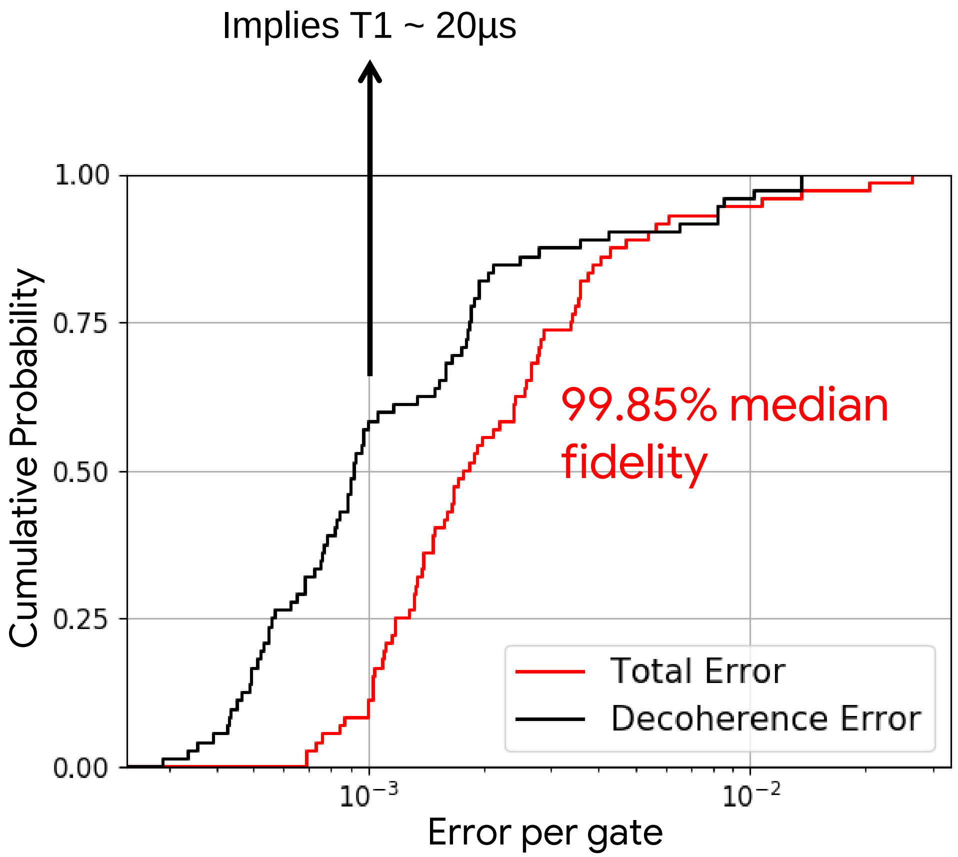

Ensemble of fidelities instead of just “best”

Google AI Quantum

2-Qubit gates

99.5% Fidelity, Arbitrary 2-qubit Gates

General model for excitation conserving gate

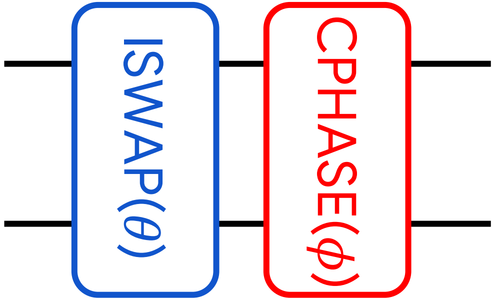

$$\begin{pmatrix} 1 & 0 & 0 & 0 \\ 0 & \cos\theta & i\sin\theta & 0 \\ 0 & -i\sin\theta & \cos\theta & 0 \\ 0 & 0 & 0 & e^{i\phi} \end{pmatrix}$$

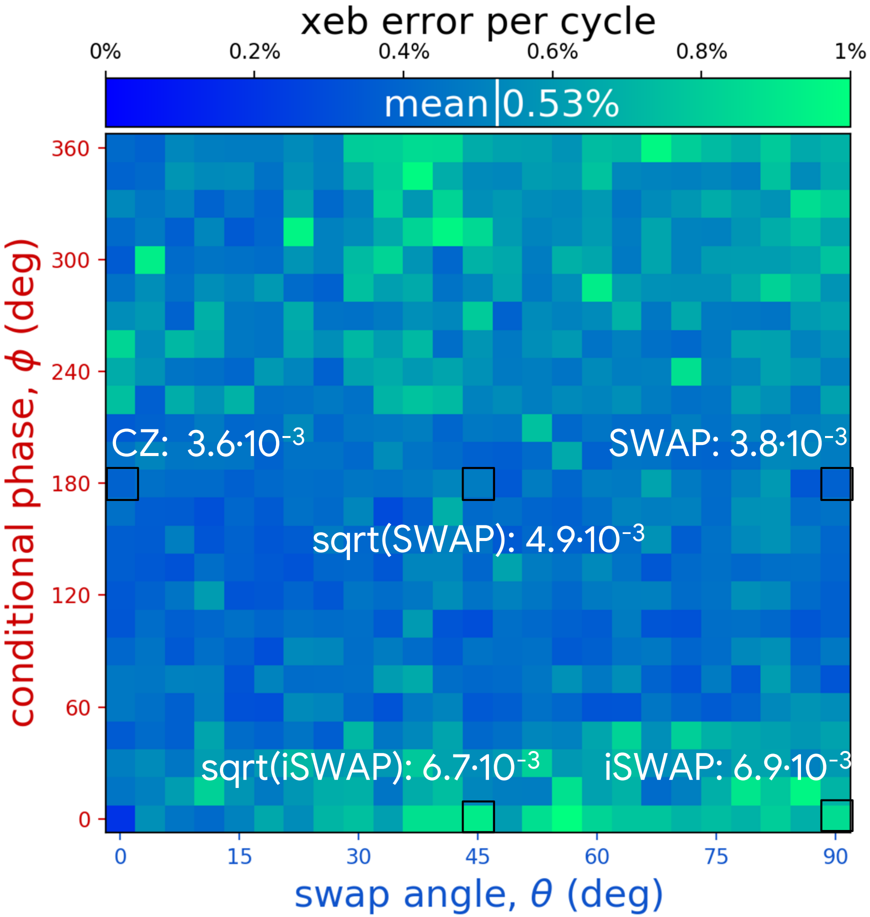

Google AI Quantum

Brooks Foxen, in preparation

High fidelity 2-qubit gates on an array

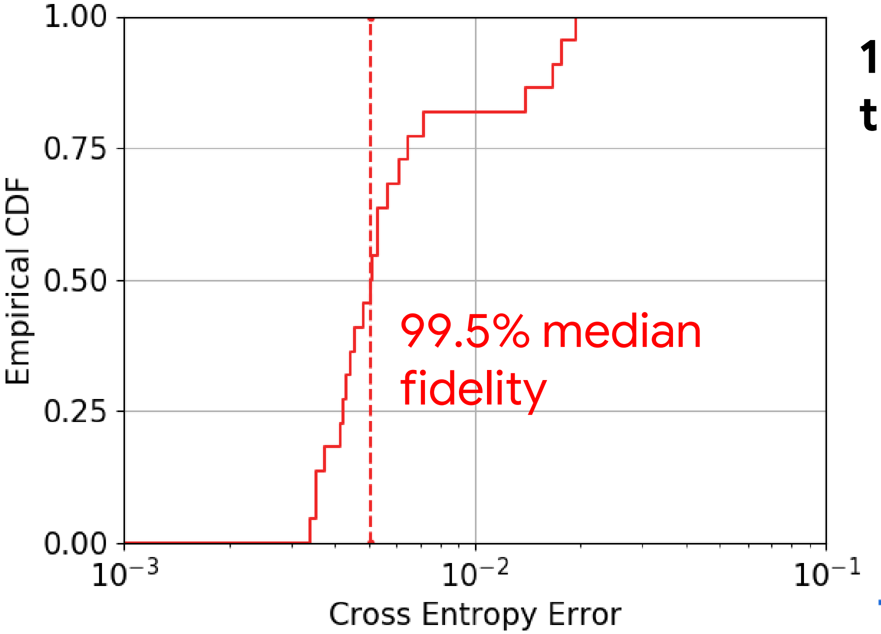

18 qubits with 22 tunable couplers

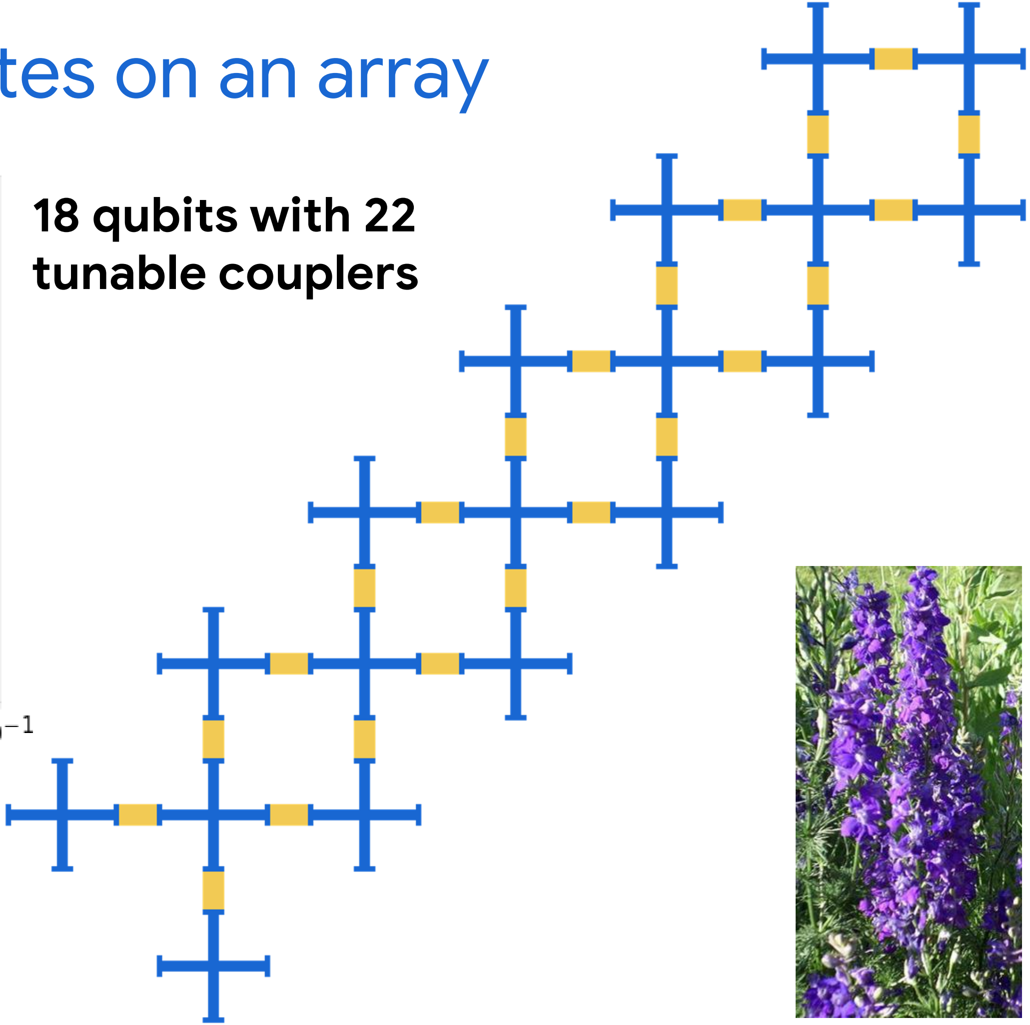

Note: Single gate for each pair of qubits, not whole subspace

Google AI Quantum

Arbitrary fSim(θ,ϕ) gate: **99.6%**

fSim(θ,ϕ)

$$\begin{pmatrix} 1 & 0 & 0 & 0 \\ 0 & e^{i\alpha}\cos\theta & e^{i\beta}\sin\theta & 0 \\ 0 & e^{i\gamma}\sin\theta & e^{i\delta}\cos\theta & 0 \\ 0 & 0 & 0 & e^{i\varphi} \end{pmatrix}$$

$|00\rangle$ $|01\rangle$ $|10\rangle$ $|11\rangle$

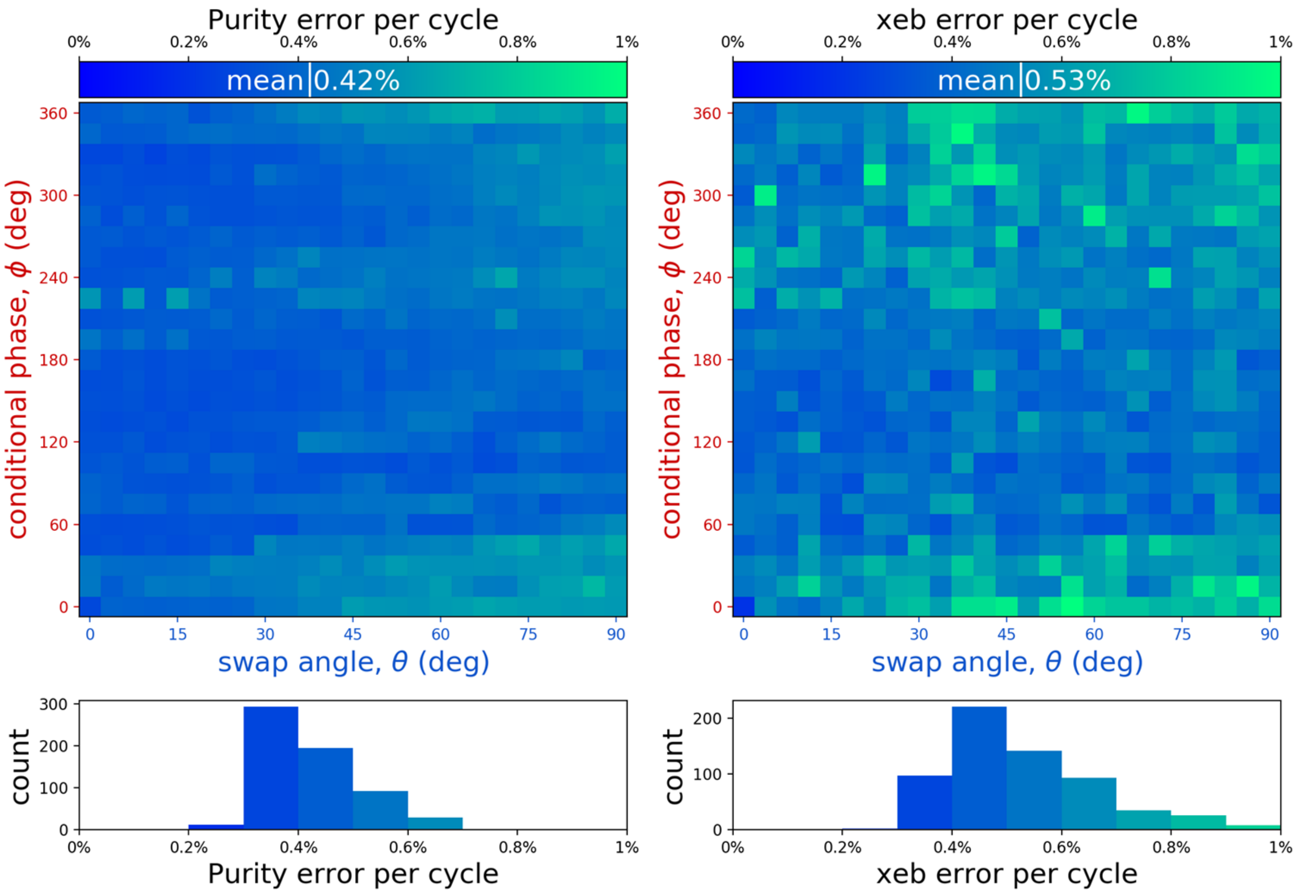

Google AI Quantum

Readout

Bristlecone - Readout

Microwave scattering for readout

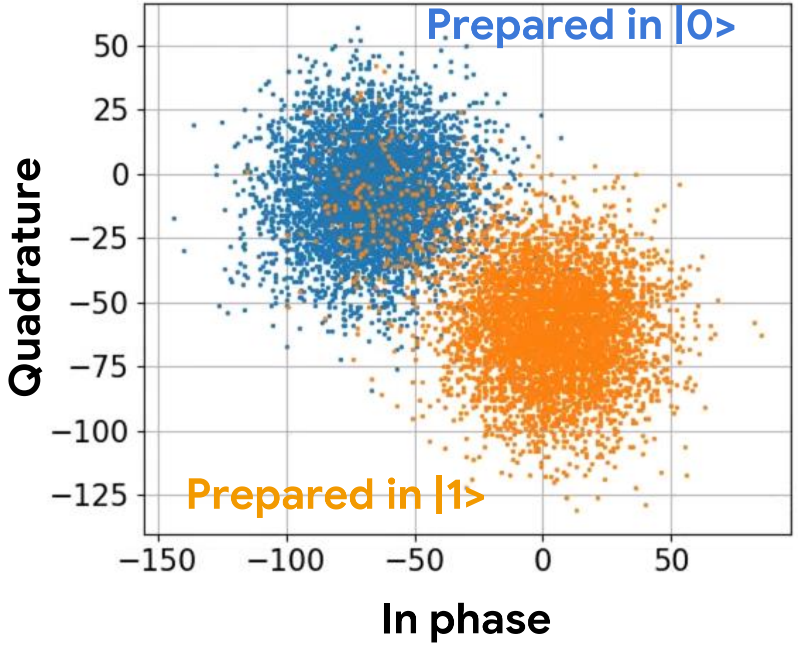

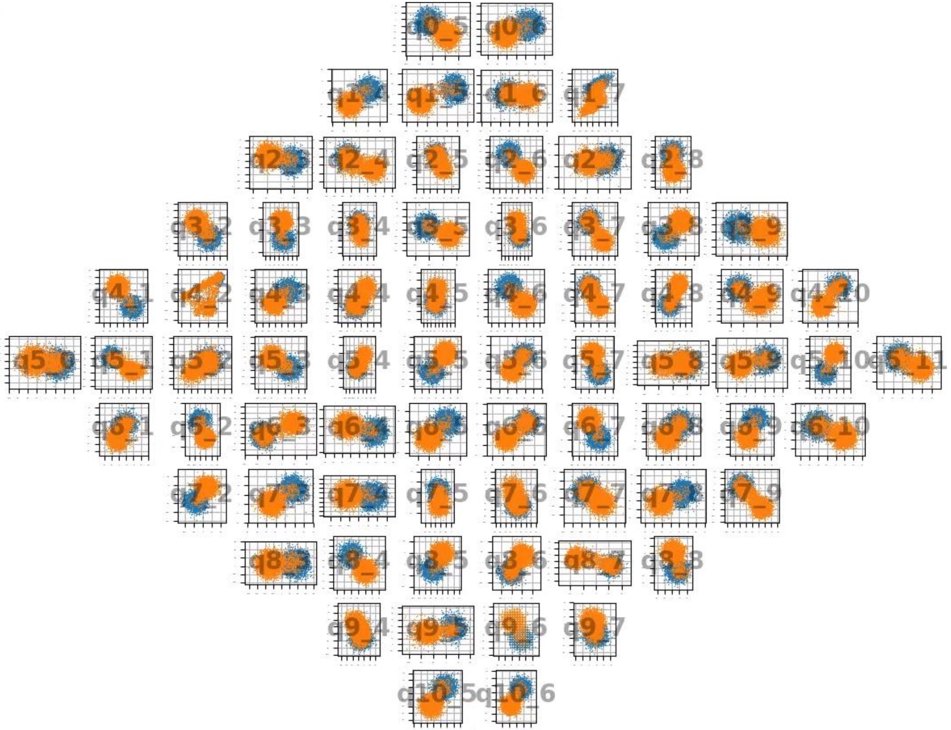

|0> and |1> discrimination for all qubits

Google AI
Quantum

Larkspur - 18 qubit device

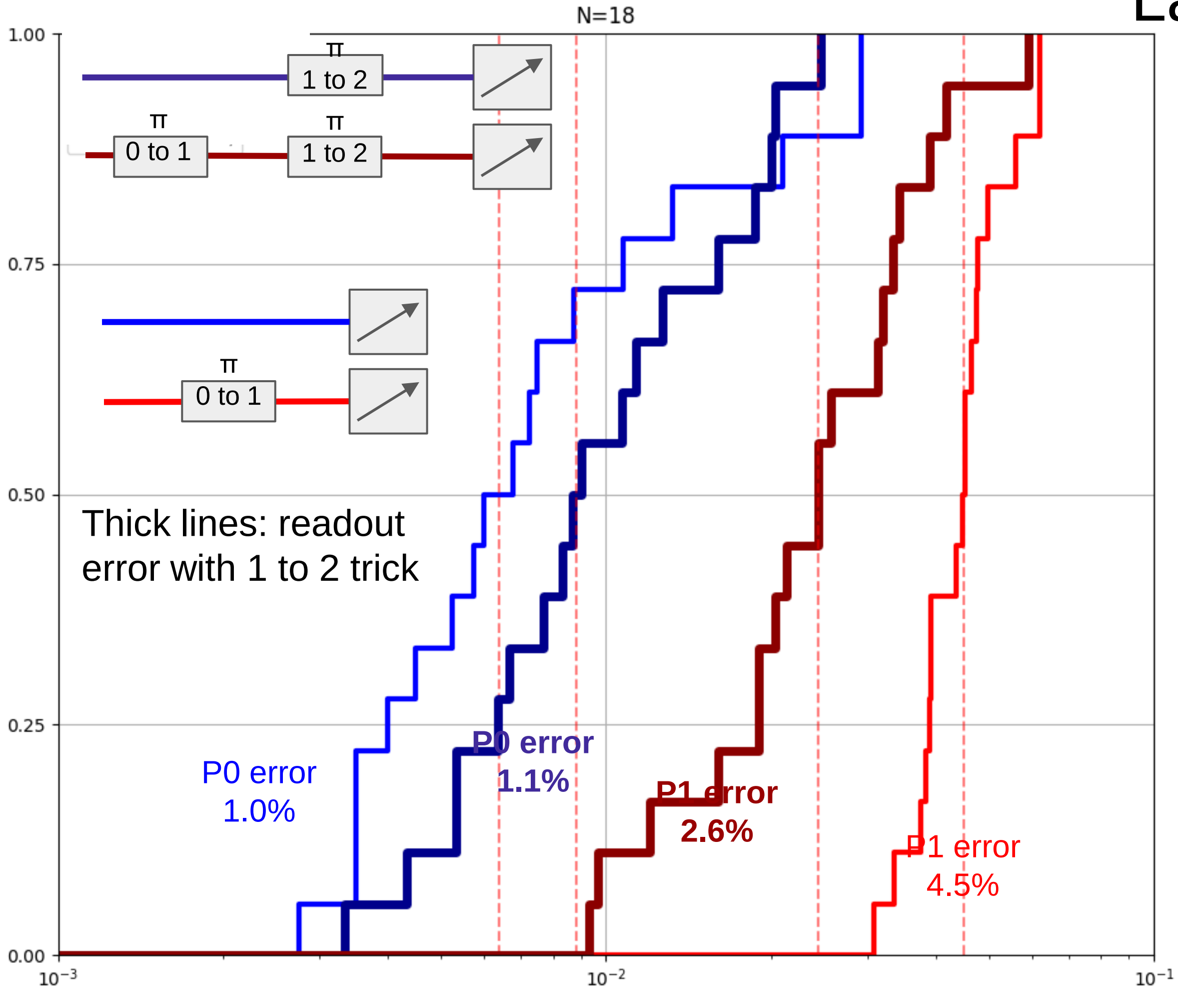

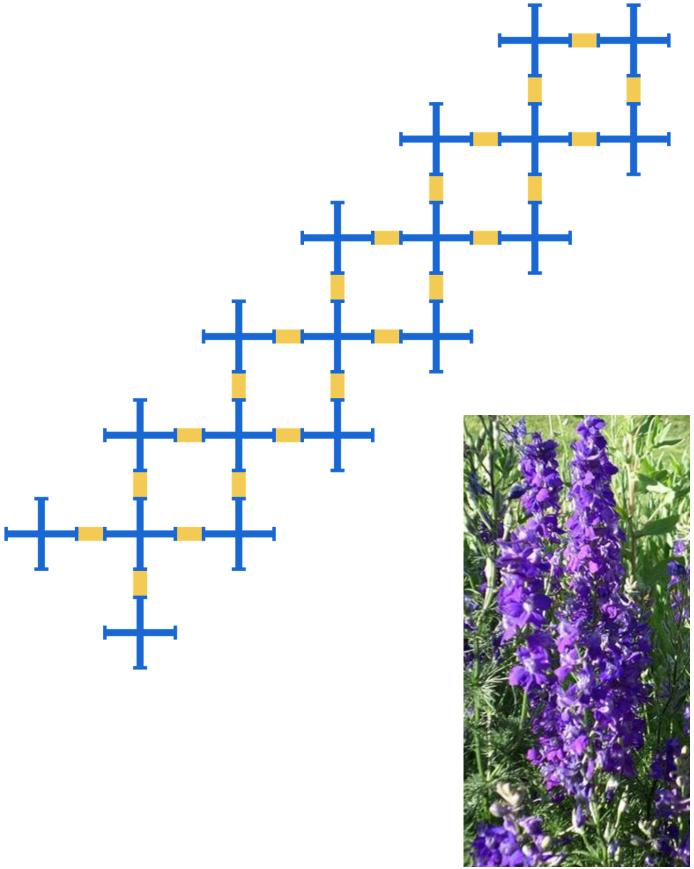

Cross talk

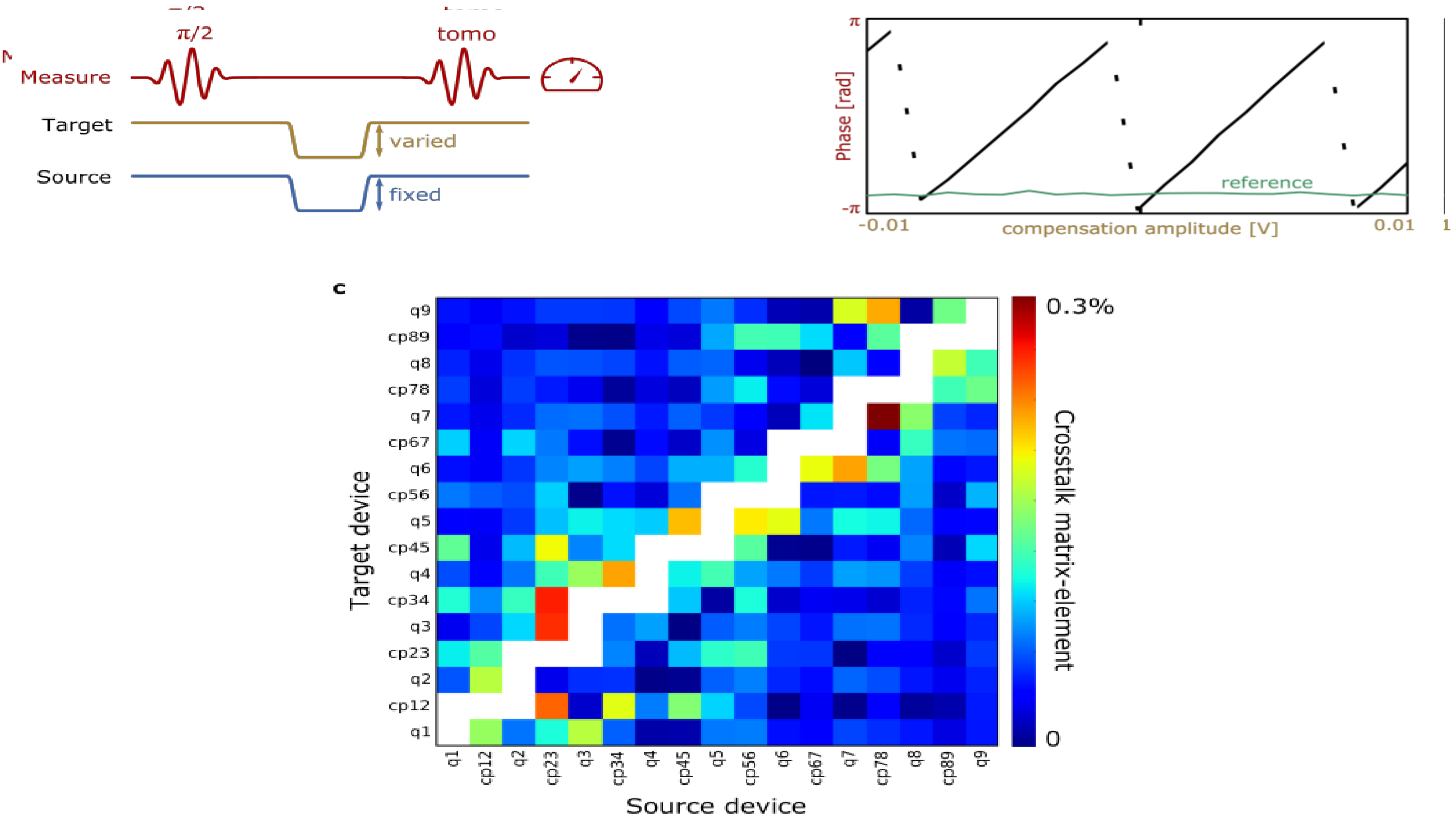
π/2
tomo
Measure
Target
varied
Source
fixed
π
Phase [rad]
reference
-π
-0.01
compensation amplitude [V]
0.01
1
c
Target device
q9
cp89
q8
cp78
q7
cp67
q6
cp56
q5
cp45
q4
cp34
q3
cp23
q2
cp12
q1
Source device
q1
cp12
q2
cp23
q3
cp34
q4
cp45
q5
cp56
q6
cp67
q7
cp78
q8
cp89
q9
0.3%
Crosstalk matrix-element
0